NOSC TR 985

AD-A 149430

NOSC TR 985

Technical Report 985

ARCTIC ACOUSTIC PROPAGATION MODEL WITH ICE SCATTERING

D. F. Gordon
Surveillance Department
Code 711

H. P. Bucker
Marine Sciences and Technology Department
Code 541

30 September 1984
Final Report
May 1983 — June 1984

Prepared for
Naval Sea Systems Command

Approved for public release; distribution unlimited

NOSC

NAVAL OCEAN SYSTEMS CENTER
San Diego, California 92152

NAVAL OCEAN SYSTEMS CENTER SAN DIEGO, CA 92152

AN ACTIVITY OF THE NAVAL MATERIAL COMMAND

F. M. PESTORIUS, CAPT, USN
Commander

R.M. HILLYER
Technical Director

ADMINISTRATIVE INFORMATION

This work was performed for the NAVSEA Arctic USW Environmental Technology Program, NAVSEA 63R, managed by Mr. D.E. Porter, under PE62759N, Subproject SF59-555. This subproject is block managed by Mr. R.L. Martin, NORDA Code 113. M.A. Pedersen of NOSC Code 711 provided technical guidance in this work.

Released by
C.L. Meland, Head
Analysis and Processing Branch

Under authority of
T.F. Ball, Head
Acoustic Systems and
Technology Division

RB

REPORT DOCUMENTATION PAGE

1a. REPORT SECURITY CLASSIFICATION Unclassified	1b. RESTRICTIVE MARKINGS
2a. SECURITY CLASSIFICATION AUTHORITY 2b. DECLASSIFICATION/DOWNGRADING SCHEDULE	3. DISTRIBUTION/AVAILABILITY OF REPORT Approved for public release; distribution unlimited.
4. PERFORMING ORGANIZATION REPORT NUMBER(S) NOSC TR 985	5. MONITORING ORGANIZATION REPORT NUMBER(S)
6a. NAME OF PERFORMING ORGANIZATION Naval Ocean Systems Center 6b. OFFICE SYMBOL (if applicable) Code 711	7a. NAME OF MONITORING ORGANIZATION
6c. ADDRESS (City, State and ZIP Code) San Diego, CA 92152	7b. ADDRESS (City, State and ZIP Code)
8a. NAME OF FUNDING/SPONSORING ORGANIZATION Naval Ocean Research and Development Activity 8b. OFFICE SYMBOL (if applicable) Code 110	9. PROCUREMENT INSTRUMENT IDENTIFICATION NUMBER
8c. ADDRESS (City, State and ZIP Code) NSTL Station, MS 39529	10. SOURCE OF FUNDING NUMBERS PROGRAM ELEMENT NO. 62759N PROJECT NO. TASK NO. RF59552 WORK UNIT NO. 712-MA43

11. TITLE (include Security Classification)
ARCTIC ACOUSTIC PROPAGATION MODEL WITH ICE SCATTERING

12. PERSONAL AUTHOR(S)
D.F. Gordon and H.P. Bucker

13a. TYPE OF REPORT	13b. TIME COVERED	14. DATE OF REPORT (Year, Month, Day)	15. PAGE COUNT
Final	FROM May 83 TO Jun 84	30 September 84	56

16. SUPPLEMENTARY NOTATION

17. COSATI CODES			18. SUBJECT TERMS (Continue on reverse if necessary and identify by block number)
FIELD	GROUP	SUB-GROUP	Acoustics, Arctic, Ice, Propagation, Scattering

19. ABSTRACT (Continue on reverse if necessary and identify by block number)

An underwater sound propagation program has been adapted to Arctic use. The program enables computation of the coherent sound field with normal modes and the incoherent surface scattered field by integrating over ray paths from the surface to the source and receiver. For Arctic use, ice scattering and ice loss functions have been developed by comparing computed losses with Arctic propagation loss data. The sensitivity of the computed losses to the form of the scattering function is determined for one frequency. A difference in ice loss between summer and winter is hypothesized, but the data are insufficient to check the hypothesis.

20. DISTRIBUTION/AVAILABILITY OF ABSTRACT [X] UNCLASSIFIED/UNLIMITED [ ] SAME AS RPT [ ] DTIC USERS	21. ABSTRACT SECURITY CLASSIFICATION Unclassified	Agency Accession DN388622
22a. NAME OF RESPONSIBLE INDIVIDUAL D.F. Gordon	22b. TELEPHONE (include Area Code) (619) 225-6301	22c. OFFICE SYMBOL Code 711

UNCLASSIFIED

SECURITY CLASSIFICATION OF THIS PAGE (When Data Entered)

DD FORM 1473, 84 JAN

UNCLASSIFIED

SECURITY CLASSIFICATION OF THIS PAGE(When Data Entered)

EXECUTIVE SUMMARY

OBJECTIVE

The objectives of this work were to (1) improve the prediction of underwater sound propagation in the Arctic Ocean by determining ice reflection and scattering losses, and (2) develop a computer model of Arctic sound propagation.

RESULTS

1. A propagation loss model has been developed for the Arctic Ocean that should be of significant value in predicting Arctic propagation performance.

2. Ice scattering losses have been determined empirically and have given good fits to three major Arctic propagation loss data sets.

3. Specifications were developed for gathering data that would distinguish between different theoretical scattering functions.

RECOMMENDATIONS

1. Introduce relative phase into scattered sound fields so that accurately modeled array performance predictions can be made.

2. Gather under-ice propagation data that will facilitate scattering determination. This requires closely spaced ranges in the first 60 km with sources or receivers spaced from above 50 m to below 400 m in depth and frequencies up to 500 Hz.

3. Use propagation loss data as they become available to update ice scattering curves used in this Arctic propagation model. Seasonal or ice condition dependence is needed.

4. Set limits on the ice scattering kernel by comparing computed losses with data.

CONTENTS

ILLUSTRATIONS

INTRODUCTION

In the Arctic Ocean, if one wishes to compute underwater sound propagation losses or to create a propagation loss model, the paramount problem is determining the effect of the overhead ice on the sound. Other aspects of sound propagation are generally easier to compute in the Arctic than in other ocean basins due to the stability of the sound speed profile and the dominance of the upward refracted, surface reflected propagation path. The acoustic effects of the ice are extremely complicated. The rough and irregular shape of the ice, its elastic properties, inhomogeneities, and even its snow cover, all affect the sound. These acoustic effects, including the parameters of the ice itself, are being ably and energetically investigated. However, while these studies are in progress, a best-available acoustic description of the ice is needed. This description can be in the form of reflection and scattering losses and scattering directions as functions of the appropriate variables. A knowledge of which variables are important is also needed.

The primary purpose of the effort reported here was to develop an acoustic description of the ice as outlined above. Our strategy was to model the non-ice dependent aspects of sound propagation as well as possible. We then sought ice reflection values that gave the best fit between computed and observed propagation loss. The results provide good general levels of ice reflection loss as functions of grazing angle, frequency, and ice roughness. Other, less definitive results that may require more data to determine or substantiate involve the functional dependence or shape of the reflection loss for the above parameters, the directional characteristics of the non-specular scatter, seasonal dependence, and ice loss as opposed to ice scatter.

A second product of this effort is an Arctic propagation loss model. This model with our ice scattering losses incorporated into it agrees well with all three major sets of data used. Samples from each set are given in this report. We chose a normal mode model that was reliable and easy to use, though necessarily range independent. That is, we must assume the environment is constant in range. The result is an Arctic model that a user can apply with ease and confidence. It can be used in both deep and shallow water, with or without ice cover. The model is discussed in the first section of this report and the input-output for two runs are given in appendix A as an aid to users in constructing runs.

Because we were interested in ice scattering effects, we chose a model with both primary and secondary scattering. Primary scattering is the loss of energy at the surface due to scattering. Secondary scattering is the propagation of this scattered energy to the source and receiver. A simple Arctic model with empirical ice loss could be constructed without using secondary scattering. However, one cannot hope to approach the true physics of the problem without accounting for the scattered energy. The use of secondary scattering in the model increases the acoustic parameters that need to be known, particularly the scattering directions or scattering kernel. It also greatly increases the information that the model can produce. The relative strength of the direct and scattered fields is an example. This is treated briefly in the final section of this report.

The scope of this study was limited by the propagation loss data that were available. For example, air-dropped explosive sources are by far the easiest sources to use in the Arctic. The data therefore tend to be sparse because the data can be gathered only from patches of open water. Also, the air drops cover long ranges; therefore the higher frequencies are greatly attenuated and tend to be neglected. We have therefore been most successful in estimating those ice acoustic effects that control the overall range dependent attenuation at frequencies of 200 Hz and below. Closely spaced and more detailed propagation loss data, when available, will permit better determination of other aspects of ice acoustics.

DESCRIPTION OF THE ARCTIC PROPAGATION MODEL

The Arctic sound field is presented as having two interacting components. There is a coherent sound field that is represented by a finite set of normal modes and a stochastic component associated with the scattered field. The normal modes are an exact solution of the wave equation when the water-ice boundary does not scatter (i.e., at very low frequencies). The number of normal modes required is a linear function of frequency with as few as 110 normal modes needed at a frequency of 100 Hz for a typical Arctic profile for long ranges.

The stochastic component of the sound field is represented by a set of integrals that are the result of sound waves interacting with the rough water-ice boundary. The scattering integrals are associated with ray paths that direct sound energy from the source to the water-ice boundary or from the boundary to a receiver (hydrophone).

A single normal mode is made of up- and down-going waves that satisfy a condition of constructive interference called the dispersion equation (ref. 1). In figure 1, the solid lines represent sound energy traveling as a single normal mode. The dashed lines represent ray paths associated with the stochastic sound field. At the source, the rays represent sound energy that travels from the source to the water-ice boundary, where scattering excites the normal mode (ray to mode exchange of energy). Near the receiver, sound energy in the normal mode is scattered at the water-ice boundary into rays that travel from the boundary to the receiver (mode to ray exchange of energy).

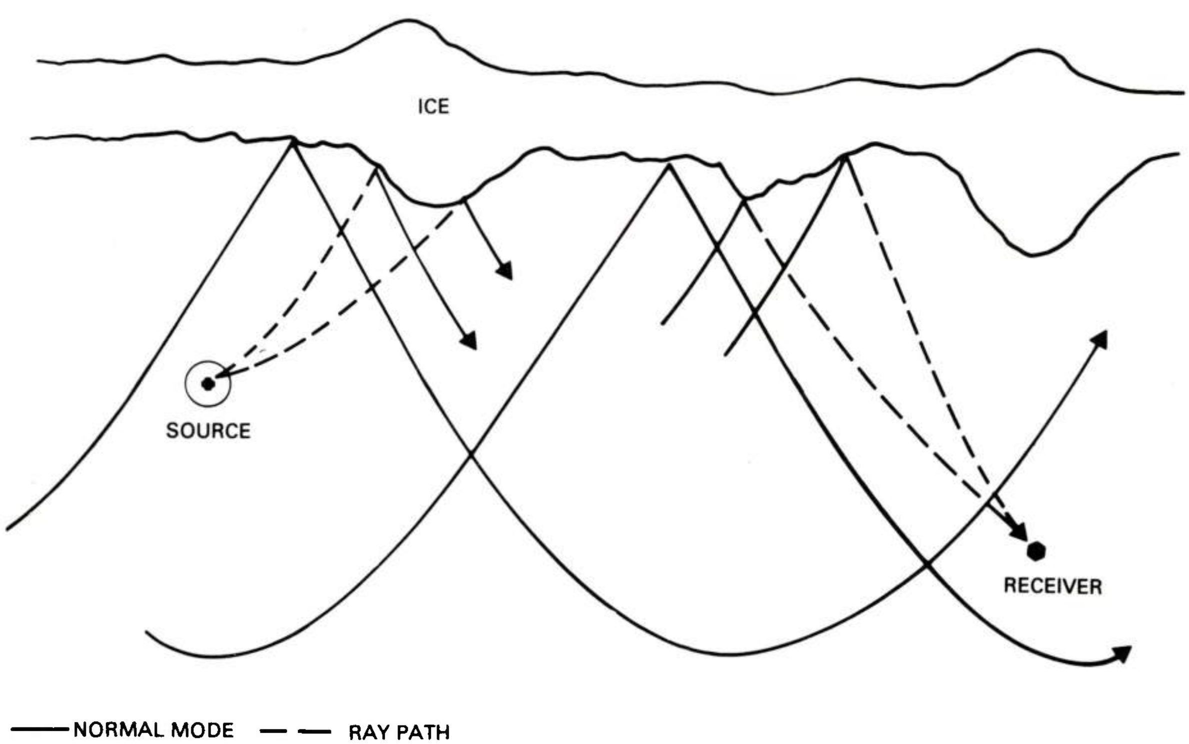

Figure 1. Mode-to-ray and ray-to-mode conversion.

In the Arctic model, the coherent field is represented as a finite set of normal modes. If P_c is the coherent field at horizontal range r and receiver depth z, then from reference 1

$$P_c = \sum_{m=1}^{M} (2\pi/r)^{1/2}\, U_m(z_o)\, U_m(z)\, \exp(ik_m r) \Big/ \left(k_m^{1/2}\, N_m\right) \tag{1}$$

In equation 1, r is the horizontal range, z_o and z are the source depth and receiver depth, U_m is the depth function which is a solution of the Helmholtz equation that also satisfies the dispersion equation, k_m is the horizontal wave number of mode m, and N_m is a generalized normalization factor. In the Arctic model, each U (depth function) can have up to 21 depth segments, or layers. Each segment of U consists of a sum of two exponential functions with + and - arguments when the sound speed is constant, or of a sum of the Airy functions, Ai and Bi, when the sound speed changes with depth (linear in the squared index of refraction). Coefficients of the exponential functions, or of Ai and Bi, are chosen so the sound pressure and the particle velocity of the sound field are continuous functions throughout the acoustic channel. The model automatically adjusts the horizontal wave number k until a value k_m is found for which $U = U_m$ satisfies the boundary conditions at the water-ice interface and at the bottom of the sound channel. The bottom condition is either the Summerfeld radiation condition, if the mode does not interact with the bottom sediments, or a bottom impedance condition if it does. This value of k (k_m) is said to satisfy the dispersion equation, and the corresponding value of U is denoted U_m.

To insure efficient computation and to eliminate the problem of not finding a normal mode, it is first assumed the k_m is real and a real k_m is found that satisfies the boundary conditions in terms of phase shifts. The imaginary part of k_m is then set by the equation (ref. 2)

$$\mathrm{Im}(k_m) = (SL_m + BL_m) \Big/ (8.686X_m) \tag{2}$$

where SL_m and BL_m are the boundary losses (in dB per reflection) at the surface and bottom of the channel, and X_m is the cycle distance (horizontal distance between surface reflections of the ray that is associated (i.e., same phase speed) as mode m.

The scattered field is written in terms of scattering integrals of the form:

$$J_m = \int_{\gamma_{s1}}^{\gamma_{s2}} [\sigma \exp(2\mathrm{Im}(k_m)\rho)/\sin\gamma_r]\, d\gamma_s \tag{3}$$

The reader should refer to reference 1 for derivation of equation 3 and for the equations that relate equation 3 to the stochastic sound field. Here, we shall show the physical interpretation of equation 3 and indicate how the integral is calculated. In equation 3, γ_s is the grazing angle of ray sound energy at the water-ice boundary, γ_{s1} and γ_{s2} are the limiting values of rays that can travel from the interface to the receiver, σ is the scattering coefficient, γ_r is the angle of the ray at the receiver, and ρ is the horizontal distance from the point where the ray is scattered at the surface to the receiver. There is also a related integral where the source replaces the receiver.

Several rays with the same γ_s contribute to the integral as shown in figure 2. Point 1 in figure 2 represents sound energy scattered at the surface (at pt. 1) and traveling directly down to the receiver. Point 2 represents sound energy scattered (at pt. 2) which is refracted back to the surface by the strong positive gradient of the sound speed in the Arctic, at point 1. This ray energy has a specular reflection at point 1; then travels directly to the receiver. Compared to the strength of the energy scattered at point 1, the energy scattered from point 2 is stronger by the factor exp $[2\mathrm{Im}(k_m(\rho_2 - \rho_1))]$, because mode m is that much stronger at point 2 than at point 1. On the other hand, the contribution from point 2 is weaker because of the specular reflection loss due to the surface reflection at point 1 and any bottom interaction loss that may occur along the path from point 2 to point 1. There are also ray paths from points 3, 4, etc., that must be included. Referring to figure 2, it is seen that there is also a set of paths with the same γ_s that arrive at the receiver from below, namely from points 1, 2, etc. These paths must be included in the integral (eq. 3) with appropriate values of ρ and corrected for specular reflection losses and bottom interaction losses, if any.

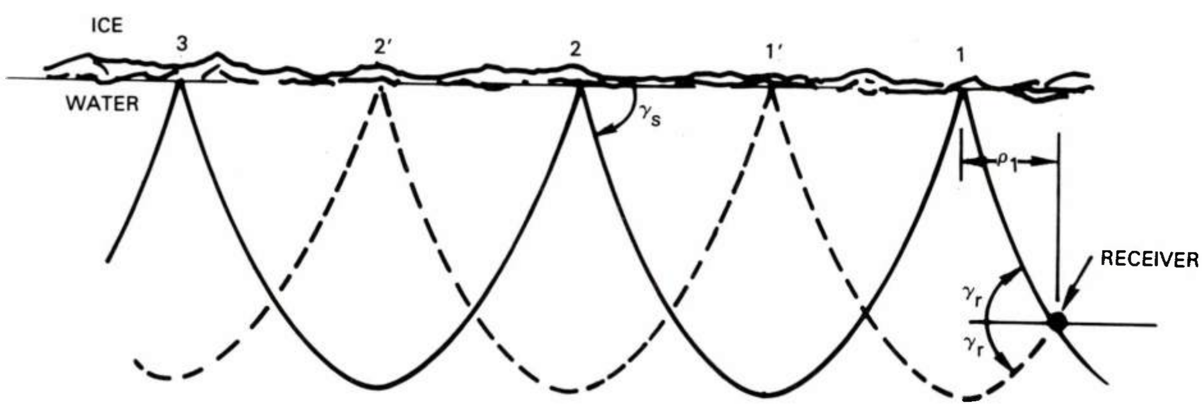

Figure 2. Ray paths from mode m to the receiver.

The scattering coefficient σ depends on the angle of the mode (or the ray of the same wave number) at the surface, the scattering angle γ_s, and the surface scattering loss. This is generally termed the scattering kernel. At present, the program uses σ proportional to sin γ_s, or Lambert scattering. The mode angle enters only in determining the total energy scattered per reflection. Only scattering in the forward direction is used. In future work we plan to determine the sensitivity of the computer propagation loss to these assumptions regarding the scattering kernel.

In summary for this section, the sound field is represented as two overlapping fields. Thus, at any point in the channel, there will be a coherent field represented by a finite set of normal modes and a stochastic field consisting of a set of scattering integrals that are associated with ray paths from the source to the water-ice interface or from the interface to the receiver. If the water-ice boundary is smooth, (i.e., r.m.s. variations of the water-ice interface $<< \lambda$, where λ is the acoustic wavelength), then σ in equation 3 will approach zero and only the coherent field will be observable. As the frequency of the sound increases, there will be more scattering and a larger stochastic contribution to that total field. On the basis of our limited experience, the Arctic model indicates an increasing stochastic field with frequency until saturation occurs, when the energy is about evenly divided between the stochastic and coherent sound fields.

ICE REFLECTION LOSS DETERMINATION

The purpose of the work reported in this section was to determine ice reflection losses due both to scattering and attenuation. The scattering is due to irregularities at the ice-water interface. The attenuation is energy that is lost at reflection and does not re-enter the water. Much of it may be by absorption of various waves in the ice. Our strategy was to use the propagation loss program described above to account for as many propagation parameters as possible. The principal unknowns are then the reflection losses. By comparing computed losses with observed losses, the reflection losses can be adjusted to give the best comparison. In this section we give the reflection loss curves that resulted from our investigation, a discussion of the data used, and finally, a discussion of the limitations that appear to be inherent in this method of determining coefficients.

REFLECTION LOSS CURVES

Figure 3 shows the reflection loss curves for two frequencies: 100 and 200 Hz. These curves give loss versus grazing angle for angles up to 20°. The curves over the shaded areas represent the reflection loss due to ice attenuation. The remainder of the loss represents scattering loss. This scattering loss is linear in decibel units for grazing angles up to 20°. The loss is 0 dB at 0° grazing angle. The scattering loss at any frequency is thus a curve of one parameter. A convenient way to express this parameter is the slope of the curve in dB/degree.

This slope of the scattering curve is a function of frequency. Figure 4 shows the frequency dependence of the slope. Note that the curve is flat above 200 Hz; i.e., the slope of the scattering loss is approximately 0.33 dB/degree for all frequencies above 200 Hz. This effect is apparently due to the scattering objects (the ice keels) becoming large compared to an acoustic wavelength. Diachok (ref. 3) demonstrates this effect and explains it using Twersky's loss scattering model. These scattering losses are determined for data from the central Arctic deep water areas. Corrections for other ice conditions will be discussed later.

ICE ATTENUATION LOSS

In figure 3, the difference between the losses caused by ice attenuation and those caused by scattering are represented by the shaded area. The ice-loss curve increases from 0 to 2 dB above the scattering curve over a 2° interval, and then remains at 2 dB above the scattering curve. These values are independent of frequency. Here, this additional reflection loss starts at 15° grazing angle. We use this value for winter ice. For summer ice we lower the starting angle to 13°. This is the only seasonal difference that we use in our reflection coefficients, and is a purely hypothetical difference. As will be shown later, it makes only a small difference in propagation loss, and very accurate data will be needed to test it. Differences in roughness of summer and winter ice may well overshadow the effect.

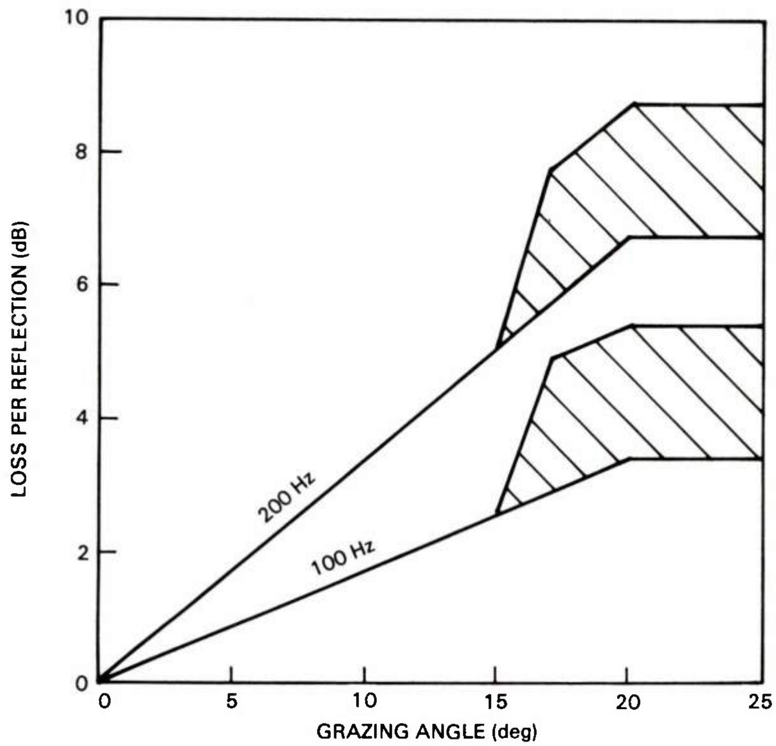

Figure 3. Ice reflection losses as a function of grazing angle at two frequencies as used in the Arctic propagation program. The losses are due to scattering except that part over the shaded area, which is due to ice loss.

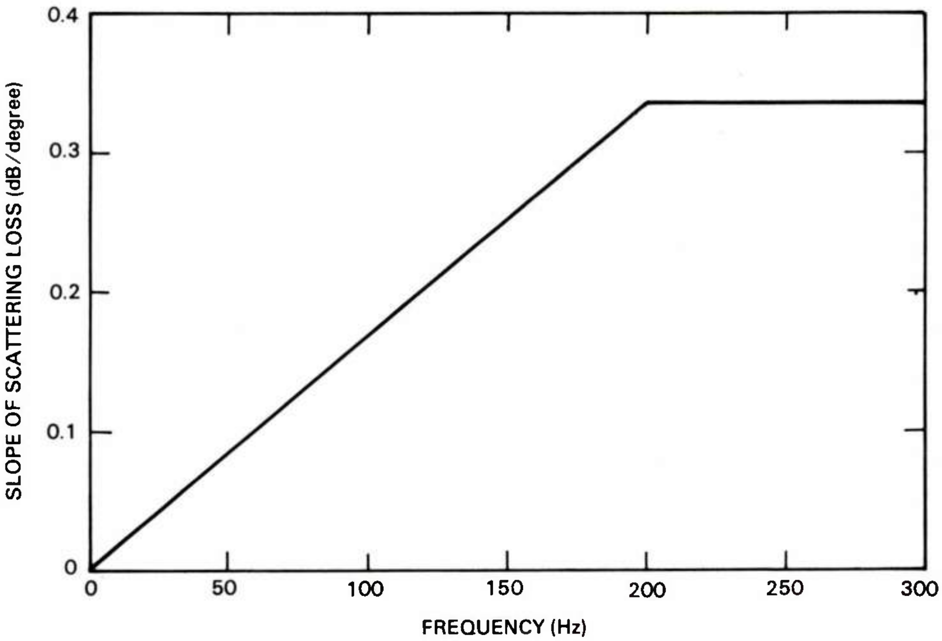

Figure 4. Slope of ice reflection loss curves as a function of frequency.

In the propagation loss model, the only difference in the use of scattering loss and ice loss is that energy lost to scattering is used in the scattering integrals and some of it reaches the receiver. The energy lost to ice attenuation is not accounted for further.

The above hypothesis regarding summer and winter ice is based on the assumption that ice loss increases abruptly when the phase speed of shear waves or surface waves (leaky Rayleigh or Sholty waves) is reached. Next, it is assumed that harder winter ice has a higher shear velocity. The only evidence on hand for these assumptions is an estimate arrived at by Mellen and Marsh (ref. 4) of a 13° ice cut-off angle. They were observing individual shot records, most probably from August-September data. Long range propagation under winter ice arrives from angles up to 17° from the horizontal. This limit could be imposed by either ocean bottom or an ice cut-off angle. In deep water, the bottom grazing rays strike the surface at about 18°. In either case, the winter cut-off angle is higher than the 13° angle of summer.

BOTTOM REFLECTIONS

Above 20°, the reflection loss curves are not important to long range propagation because rays that strike the surface at this angle also strike the bottom. These rays strike the ice at relative short range intervals and are rapidly attenuated. To use our current technique to determine reflection losses at these angles would require both carefully observed losses along bottom reflected paths and very reliable bottom loss coefficients. Neither of these requirements have been available in this study.

We have used a reasonable set of bottom reflection loss curves. Those at four frequencies are shown in figure 5. These curves were determined from normal mode theory using a fluid bottom with a sound speed gradient of 1.0, a density of 1.8 gm/cm^3, and sound speed is continuous at the water-sediment interface. The curves are arbitrarily continued at higher angles that have little effect on long range propagation.

ICE ROUGHNESS DEPENDENCE

Finally, the reflection coefficients just given must be adjusted for ice roughness. We have followed Buck in expressing ice roughness in terms of the standard deviation of ice depth, s. Figure 6, published by Buck (ref. 5) from LeShack and Chang (ref. 6) shows contours of s on a map of the Arctic Ocean. Data from which our loss curves were calibrated came from areas of s approximately equal to 2 meters, and the previously presented loss curves are assumed to be for s = 2m. Curves for several values of s are given in figure 7. These curves are based on relatively small samples of data, as will be discussed later. A simple algebraic form that fits the scant data has been selected as follows: letting the slope of the curve at s = 2 be K(2, f) and

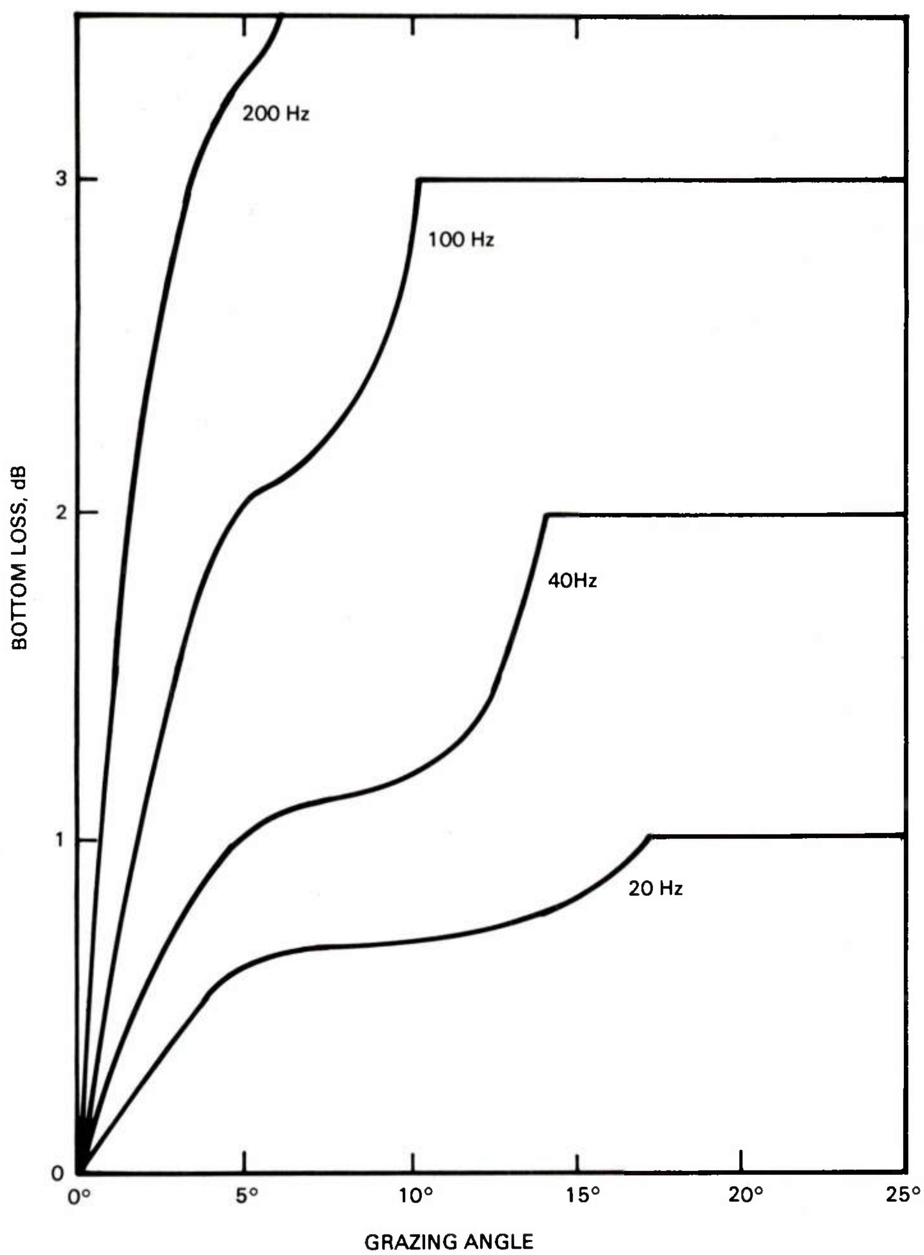

Figure 5. Bottom reflection loss as a function of bottom grazing angle for four frequencies.

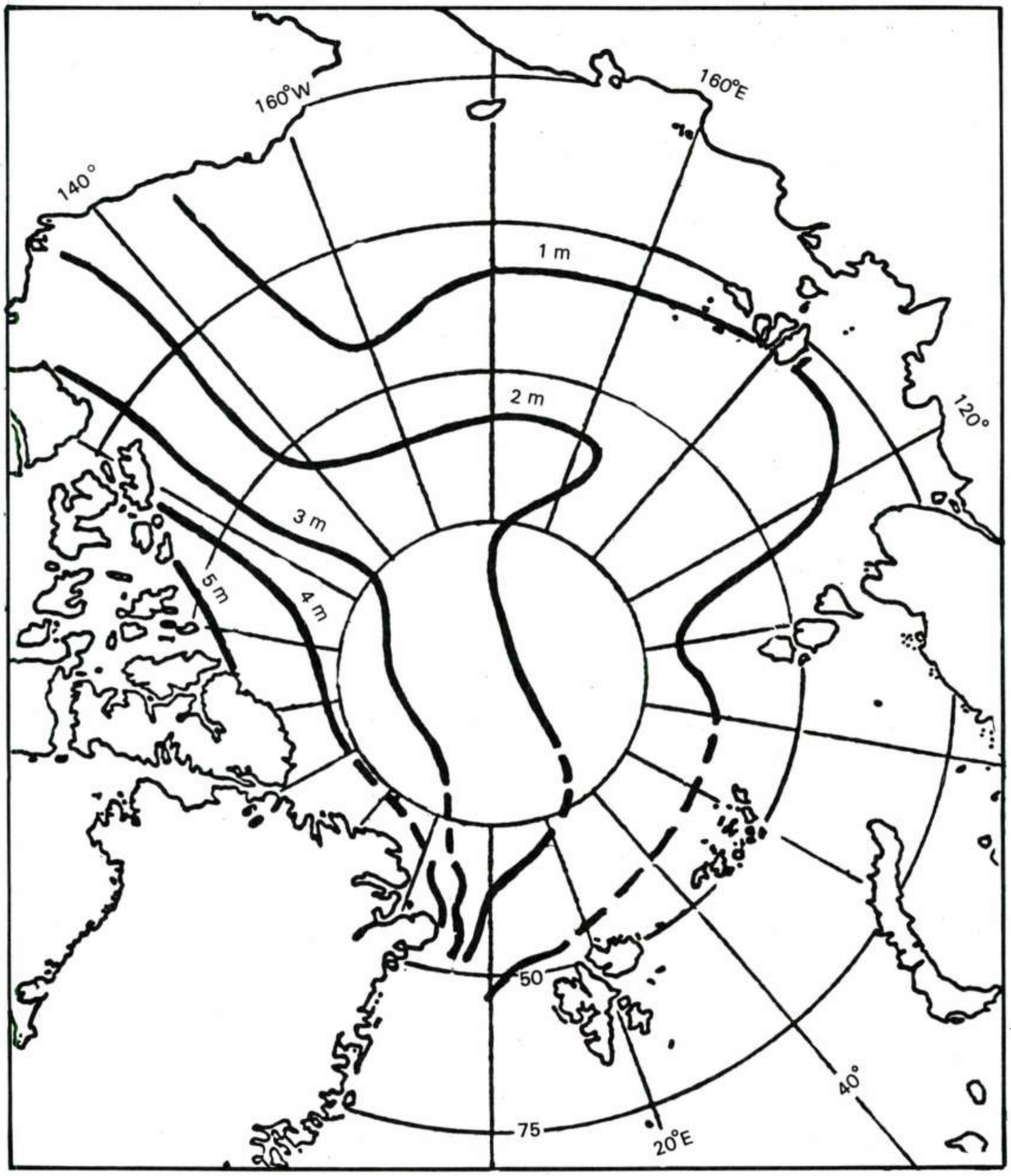

Figure 6. Contours of standard deviation of ice depth in meters from LeSchack and Chang.

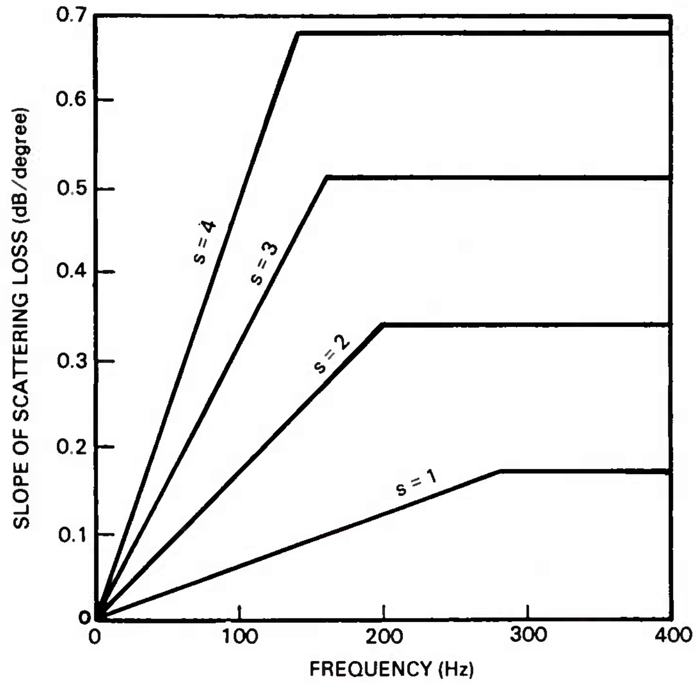

Figure 7. SLope of ice scattering loss curves as a function of frequency and of s, the standard deviation of ice roughness.

the saturation frequency at which scatters are large compared to a wave length be f_o, our curves are expressed as:

$$K(s,f) = (s/2)^{1.5} K(2,f) \qquad f_o \le 200(2/s)^{0.5}$$

$$K(s) = (s/2)^{1.5} K(2,f_o) \qquad f_o > 200(2/s)^{0.5} \tag{4}$$

Inserting the value for the slope at s = 2 m from figure 2, the scattering loss slopes are

$$K(s,f) = 0.000597\ fs^{1.5} \quad \text{dB/degree/Hz} \qquad f \le 283s^{-0.5}$$

$$K(s) = 0.169s \quad \text{dB/degree} \qquad f > 283s^{-0.5} \tag{5}$$

FITTING PROPAGATION LOSS DATA

The scattering loss curves of the previous section were derived by selecting values of slope which gave best overall fits to certain published Arctic propagation loss data. The fits to these data are shown next. In determining all fits, we used the sound speed profile shown in figure 8. Except where noted, a water depth of 3500 m was used. Sample bottom reflection losses were shown in figure 5. Thorp volume attenuation was used throughout. Except where noted, the data are assumed to be April-May data, and hard winter ice is assumed. That is, the ice loss curves start at 15° grazing angle as in figure 3. Ice depth standard deviation is 2 m.

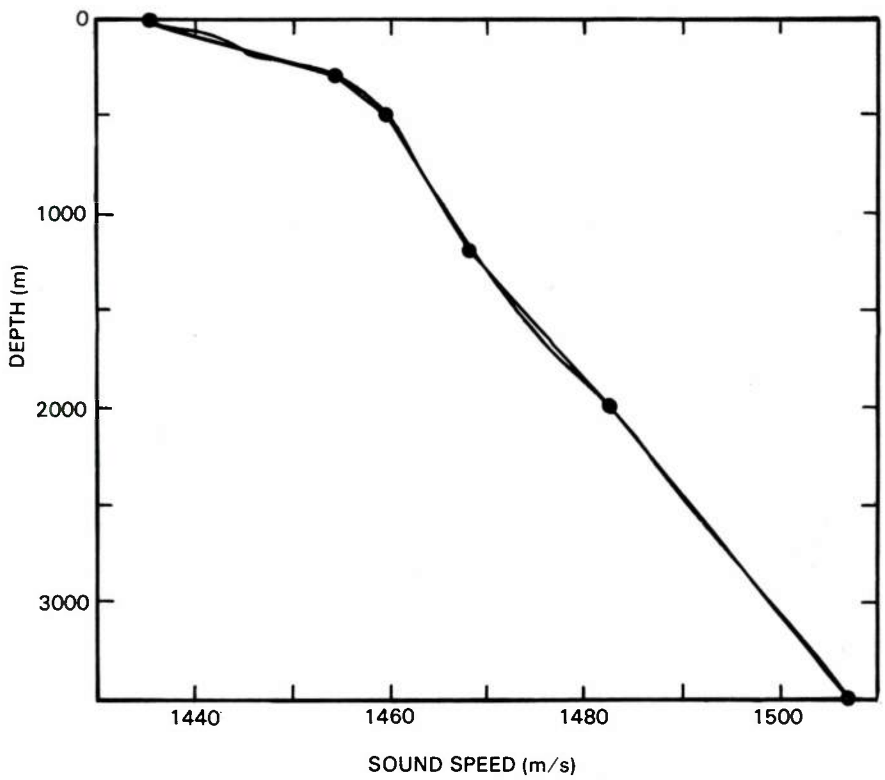

Figure 8. A five-layer approximation to a typical Arctic sound speed profile.

DIACHOK'S DATA

The most consistent data set available to us was that published by Diachok (ref. 3) for the "smooth" ice case (tracks 22 and 26). Two frequencies, 50 and 200 Hz, were used. The fits to these data are shown in figures 9 and 10. Because of the consistency of these data, we required a close fit. The fits were made by eye, by matching the propagation loss curves to the published data. The data were not available in digitized form for computer processing.

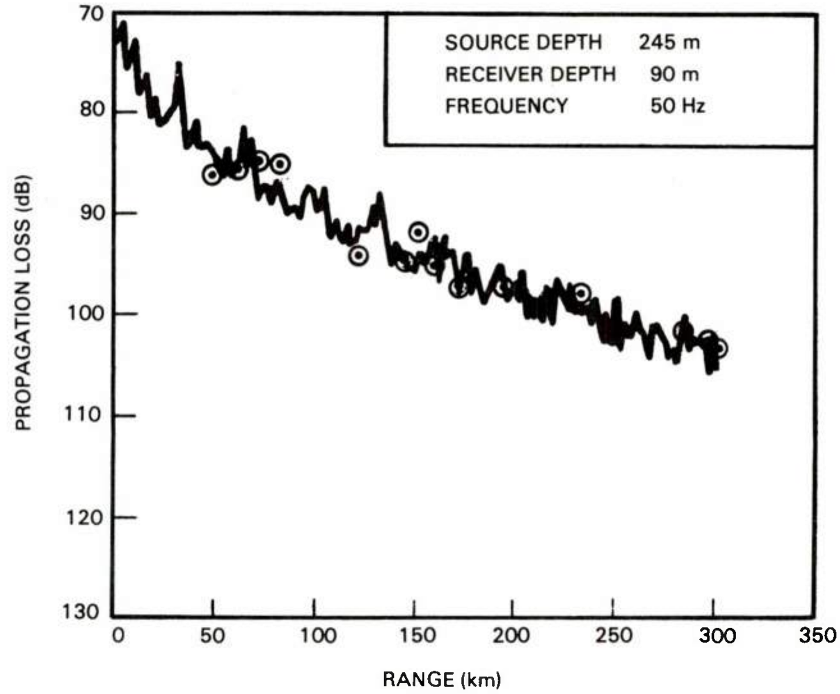

Figure 9. Comparison of Arctic shot data at 50 Hz with computed propagation losses. Data from Diachok.

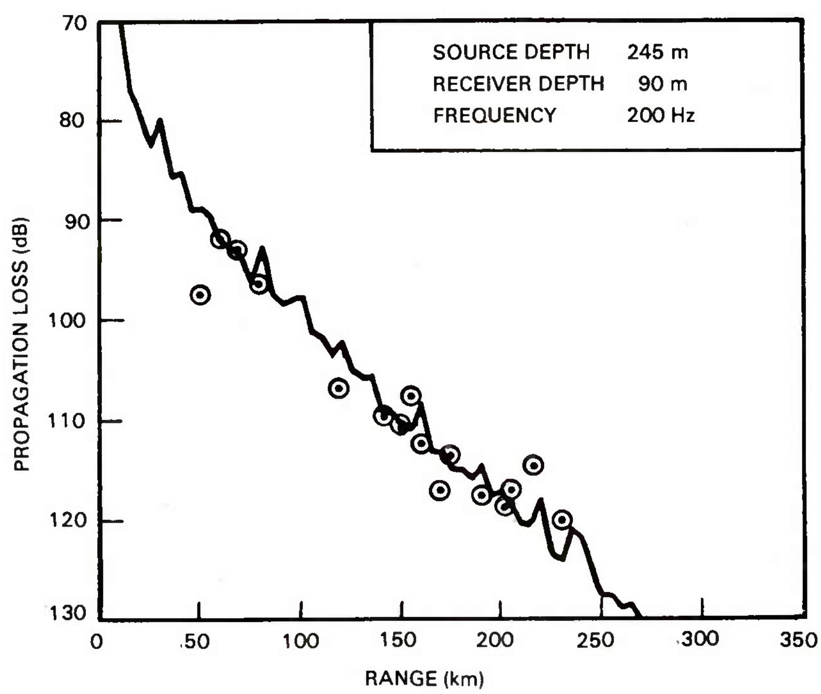

Figure 10. Comparison of Arctic shot data at 200 Hz with computed propagation losses. Data from Diachok.

BUCK'S DATA

Data published by Buck (ref. 5) were apparently derived from more diverse observations, but were for a single shot depth and a single receiver depth, as printed on the figures. Buck states that data for shallow paths have been excluded from the set. The data include frequencies from 10 to 200 Hz. Figures 11 to 13 show fits for 50, 100, and 200 Hz. The computed losses differ from those of the previous figures only in receiver depth. The circles in the figures represent shot data and the crosses are from cw data.

In these three plots, there is a tendency for the computed losses to be above the data at intermediate ranges and below the data at longer ranges. This may indicate a shortcoming in our reflection loss curve, which is linear in decibels. This will be discussed later. However, this interpretation is not compelling, and a simple scatter of the data is also a possible interpretation.

MELLEN AND MARSH DATA

The third set of data available to us was that of Mellen and Marsh (ref. 4). These data were taken predominantly in 1959 and 1962 from Fletcher's Ice Island (T3) and are of a more varied nature than the previous sets. Source depth, receiver depth, and shot yields varied. The presence of the ice island at the receiver may have introduced a consistent increase in loss into the data. This ice island might also have been the source of the 13° ice cut-off angle that we have attributed to summer ice. The greatest source of variation in the loss data is almost certainly the ocean depth. The ice island was in water of less than 1000-m depth when much of the data were gathered. Assuming that shallow water along the propagation path is more likely to increase loss than to decrease it, we have chosen to fit our loss curves to the less lossy data points.

Figures 14 to 16 show fits to the Mellen and Marsh data at frequencies of 100, 200, and 800 Hz. These data are particularly useful in giving us some higher frequency points to tie down the high frequency end of the reflection loss curves.

ICE ROUGHNESS

The ice roughness dependence of our reflection loss function was determined with considerably less precision than the frequency dependence. This is because fewer data sets were available, and also because knowledge of s (the ice depth standard deviation) to attribute to the data sets was far from certain. The following data were employed. Diachok's (ref. 3) "rough" ice cases (tracks 18 and 20) were used with s = 3.5 m. Buck's empirical fit gave a good functional relationship between s and propagation loss for frequencies between 10 and 100 Hz. Finally, Milne's (ref. 7) data were tried. These last data were of little real value to us because the experimental track extends from water of 500- to 1300-m depth. Our constant depth model cannot be used with confidence for such a path. Nevertheless, a computation using a depth of 700 m and s = 4.5 m showed good agreement with the slope of the data at 100 Hz.

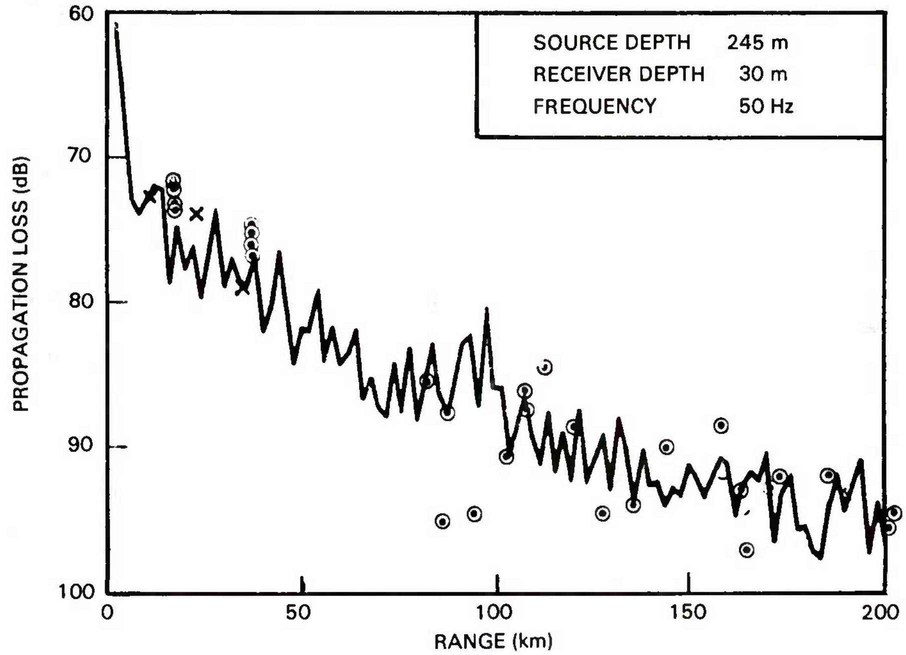

Figure 11. Comparison of Arctic shot and cw data at 50 Hz with computed propagation losses. Data from Buck.

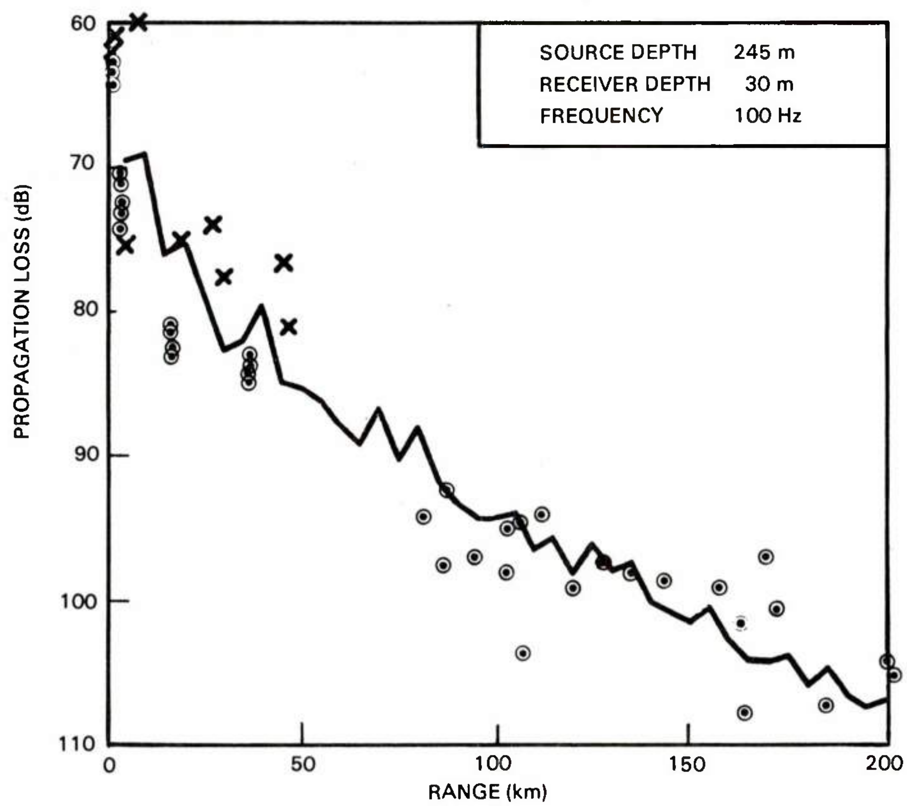

Figure 12. Comparison of Arctic shot and cw data at 100 Hz with computed propagation losses. Data from Buck.

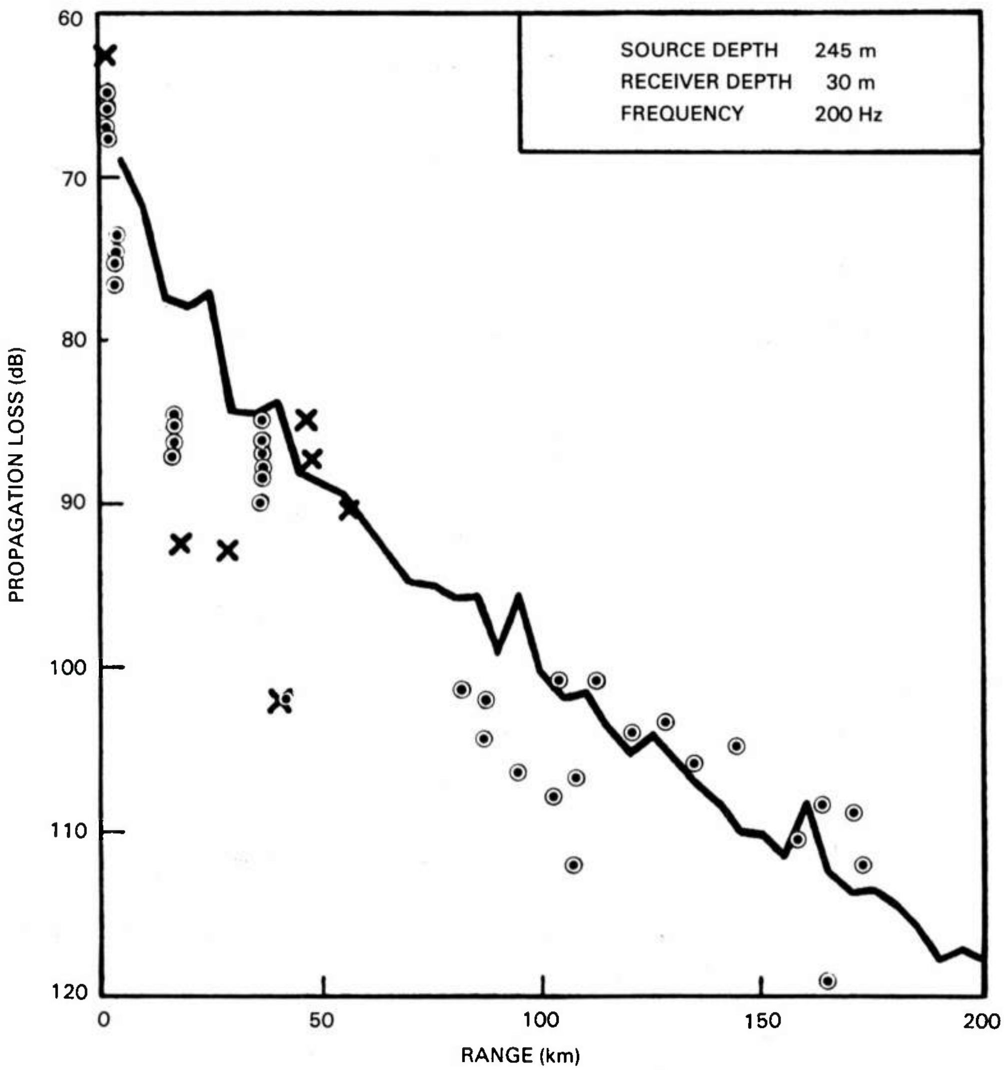

Figure 13. Comparison of Arctic shot and cw data at 200 Hz with computed propagation losses. Data from Buck.

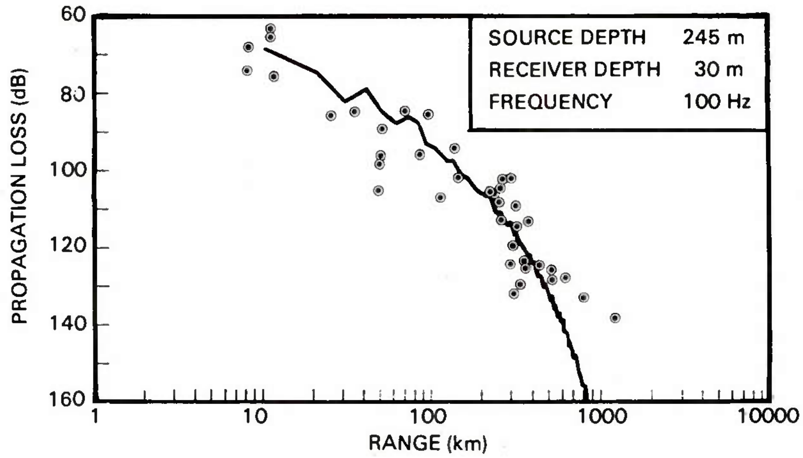

Figure 14. Comparison of Arctic shot data at 100 Hz with computed propagation losses. Data from Mellen and Marsh.

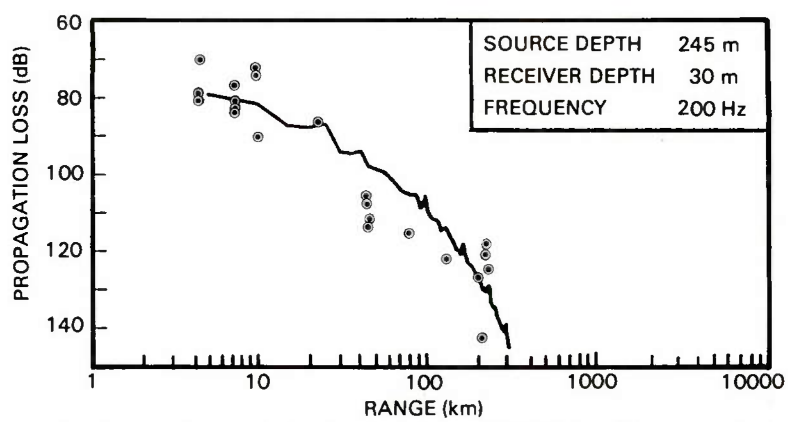

Figure 15. Comparison of Arctic shot data at 200 Hz with computed propagation losses. Data from Mellen and Marsh.

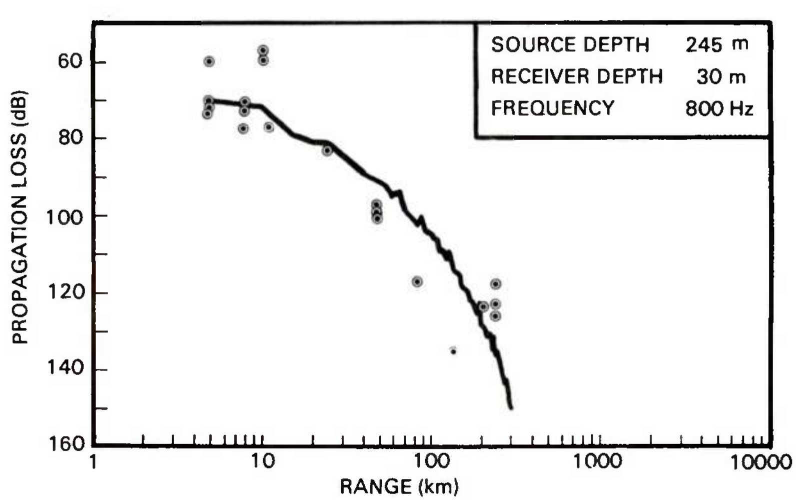

Figure 16. Comparison of Arctic shot data at 800 Hz with computed propagation losses. Data from Mellen and Marsh.

Figure 17 shows the fit using the Milne data points as plotted by Mellen and Marsh (ref. 4).

The slope of the computed and observed losses agrees well, but there is a consistent 7-dB offset beyond the first two data points.

The above data represent a small number of points upon which to base the ice-roughness dependence of our curves. This dependence should therefore be considered tentative, pending the availability of more data. Of course, our overall strategy of determining reflection loss curves is data dependent. The curves are therefore expected to change as additional data are used to verify and update them.

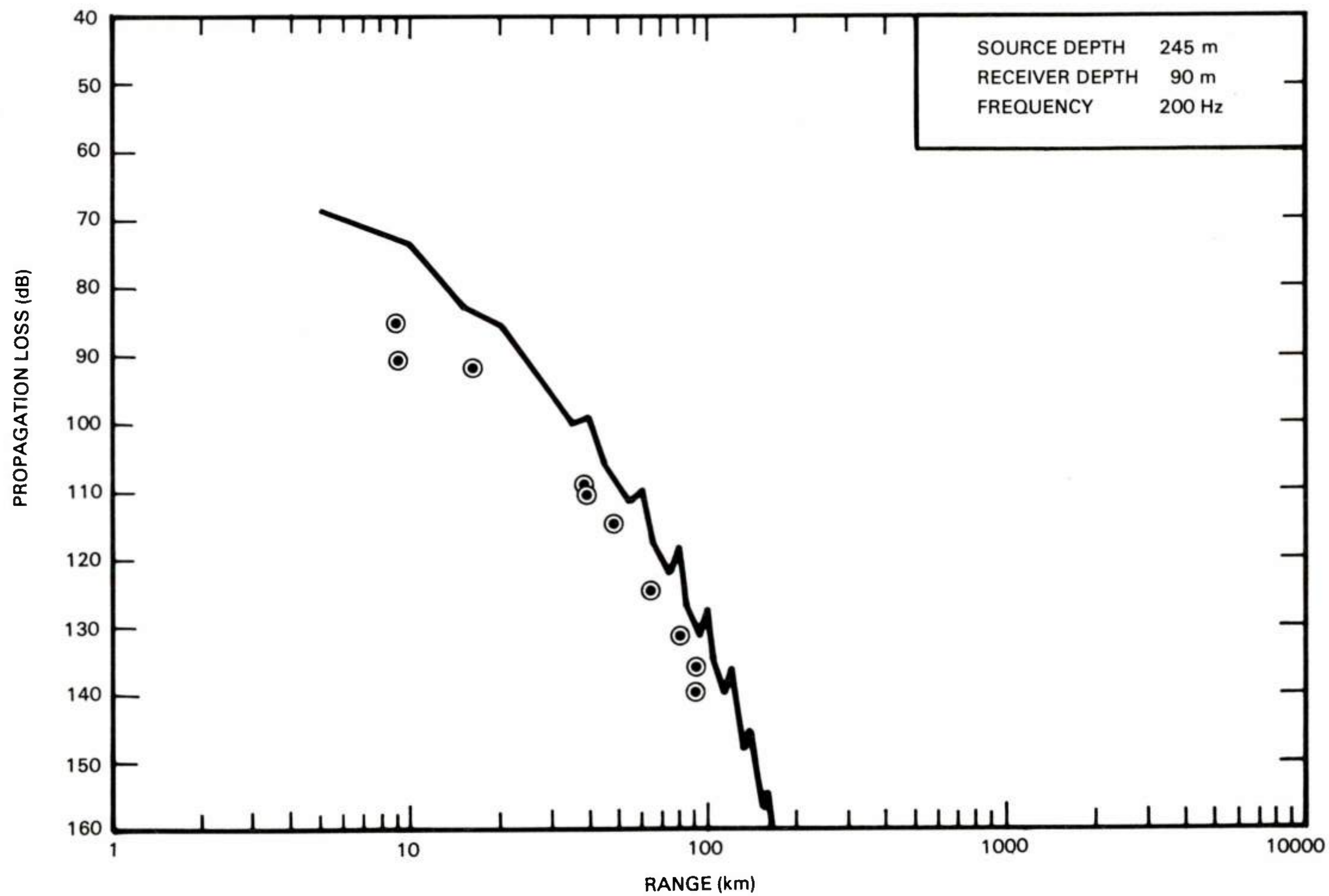

Figure 17. Comparison of Arctic shallow water shot data with computed propagation losses using s = 4.5 m. Data from Milne.

COMPARISON OF REFLECTION LOSS FUNCTIONS

The simple scattering loss functions of figure 7 lead to good agreement between observed data and computed losses. They give some general information on the functional dependence of the losses. In the following, we investigate these dependences further.

PROPAGATION LOSS FOR DIFFERENT SCATTERING FUNCTIONS

We chose a linear function for loss versus grazing angle because of its simplicity. In this section we will compare this function with other possible forms. Our ultimate purpose is to determine if the form of the function makes sufficient difference in the computer losses to permit selection of the best form by comparison with data. Alternatively, we should determine how good or how much data is required to distinguish between the different reflection loss curves. To distinguish, the standard error of estimation of a least squares fit to the data should be less than the differences produced by computing losses with different forms of the reflection loss curves. Here we will show one determination of this difference. Making least squares fits to data is left to the future.

Figure 18 shows four forms for the reflection loss curve for 100 Hz. They are all made equal at 12° gazing angle. Rays near this angle have the smallest attenuation due to surface loss when the linear reflection loss curve is used. The curve titled "log linear" is our linear in decibels curve. Diachok (ref. 3) uses two forms of Twersky's reflectivity. For low frequencies, the curve is linear in intensity and the curve of this form is the "intensity linear" curve. At high frequencies, Diachok uses a rational expression which gives the "high frequency" curve. We fit this curve to our common point at 12° by choosing a value for one of the parameters, x, of 0.7. The final curve is a constant. The frequency of 100 Hz is an intermediate value to which neither Twersky's low nor high frequency limits apply.

Figure 19 shows losses computed for these four curves. The modes have been added in random phase to suppress the mode interference beats so that the four loss curves can be compared. The difference can be seen more clearly in figure 20, where the difference between losses for the log linear curve and each of the other three is plotted. Clearly, the curve of greatest difference from the log linear curve is the high frequency curve. The greatest difference between the computed losses at 40 and at 200 km for these two curves is 10 dB. Such differences could be clearly distinguished in an experiment designed to elucidate them.

The losses for the constant reflection curve are intermediate between the log linear and the high frequency losses. The intensity linear losses differ little from the log linear, and one can be used as well as the other for practical computations.

The propagation losses of figure 19 were computed for source and receiver, both at 50-m depth. When a source depth of 245 m was used, as in much of the data given here, the differences in propagation loss between the four functions were much reduced. The reason is that shallow paths that strike the surface at grazing angles below 8° do not reach the deeper sources. It is

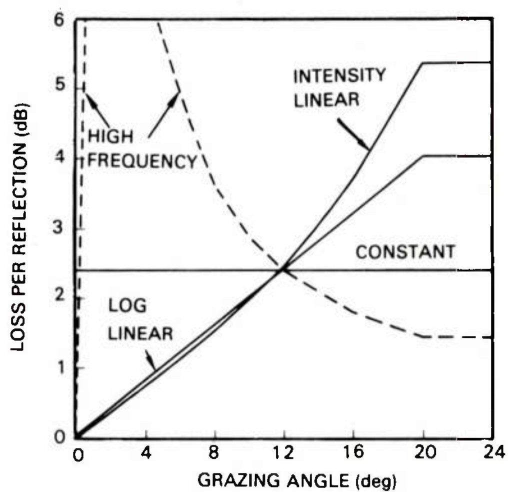

Figure 18. Four candidate reflection loss curves.

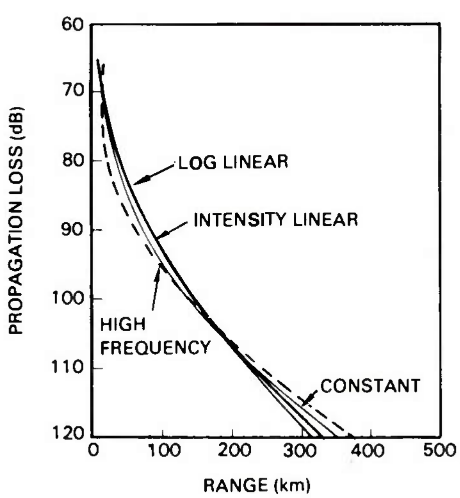

Figure 19. Losses computed for the four reflection loss curves of Figure 18 at 100 Hz.

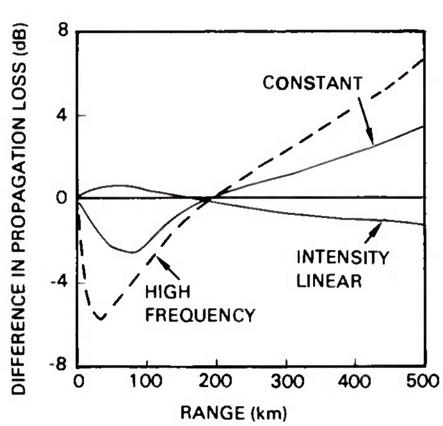

Figure 20. Differences between the loss curves of Figure 19.

these paths where the different loss functions discriminate most. When these paths are not included, the discrimination between the different functions is lost. Figure 21 shows path depth or ray vertexing depth as a function of surface grazing angle for the Arctic profile used here. For a given source or receiver depth, rays with surface grazing angles less than that shown in the figure will pass above the source or receiver. Only diffracted or scattered energy from these shallower paths will be propagated.

This need for shallow source and receiver means that the data given here, such as that of figure 12, are not effective for distinguishing between different scattering curves. It further indicates that an experiment designed to indicate something about the scattering curves should have a shallow source and receivers.

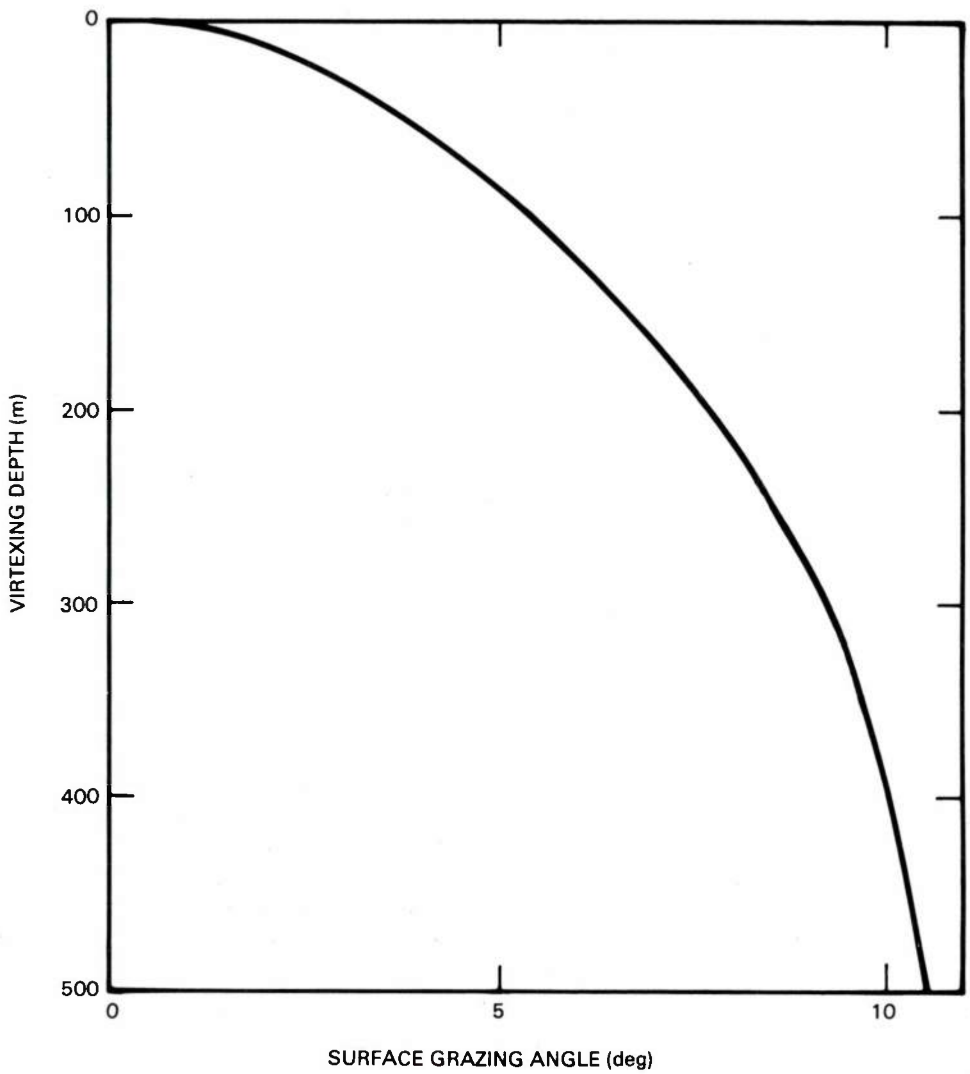

Figure 21. The depth at which rays of given surface grazing angle vertex for the Arctic profile of Figure 8. The ray is confined between this depth and the surface.

DIFFERENCE IN SUMMER AND WINTER COMPUTATIONS

As stated earlier, this computer model distinguishes between winter and summer ice by placing the leading edge of a 2-dB ice loss function either at a 13° or 15° grazing angle. The ice loss was illustrated by the shaded area in figure 3. The ice loss was implemented in hopes that ice cut-off angles could be elucidated by comparing computer runs with observed data. In the following, we compare runs that differ only in this way and show that the difference is small. It appears that reliable values of ice loss will have to be determined in other ways, and that their inclusion in the program will not greatly alter its output.

Figure 22 shows the difference in decibels between computations using three different values for the leading edge of the ice loss function. They are expressed as differences in propagation loss from the 15° value that is the standard used in this report. The exception was 13° for the Mellen and Marsh data. At 500-km range, the use of the 13° value increases the loss by 2.7 dB. A similar increase in loss could be obtained by changing the s (standard deviation of ice depth) from 2 m to 2.1 m, and thus altering the scattering loss by 8 percent. This difference in s is too small to be readily measured in the Arctic, making an experimental verification unlikely. The difference in the shape of the 13° curve in figure 20 from a straight line might be used. As in the previous section, one would compare computed and observed losses at 40 km with those at some long range to get the greatest sensitivity. However, only about 1 dB difference is predicted between the 13° and 15° cases when scattering losses are adjusted to give best fits. Propagation data are not likely to distinguish between such small differences.

The 20° line on figure 22 is almost equivalent to removing the ice loss completely. Rays of 17.6° or greater grazing angle will be bottom reflected for the 3500-m depth used in these computations. These rays contribute almost nothing at long ranges. Even at shorter ranges, their ice scattering and bottom loss, compounded by short skip distances, produce a high attenuation rate and an additional 2 dB per bounce due to ice loss which is difficult to measure.

REFLECTION LOSSES FOR MODELS WITH FIRST ORDER SCATTERING

Some users may wish to use the reflection coefficients given here in a program with only first order scattering. That is, energy is lost at the water-ice interface but is not returned to the sound field by some computation such as the scattering integrals used here. This returned energy is called secondary scattering. To obtain equivalent fits to the data, such a program should use smaller values of reflection loss. Here we show that using a scattering loss in decibels that is 0.75 percent of the losses presented in this report gives reasonable agreement. However, the two types of computations have different source-receiver depth dependence and the agreement is only approximate.

Figure 23 is a repetition of figure 12 with a second loss computation added. This added computation is the propagation loss using 0.75 percent of the scattering loss of figure 3 and using no secondary scattering. This is accomplished in the program by placing all the surface loss in the ice loss

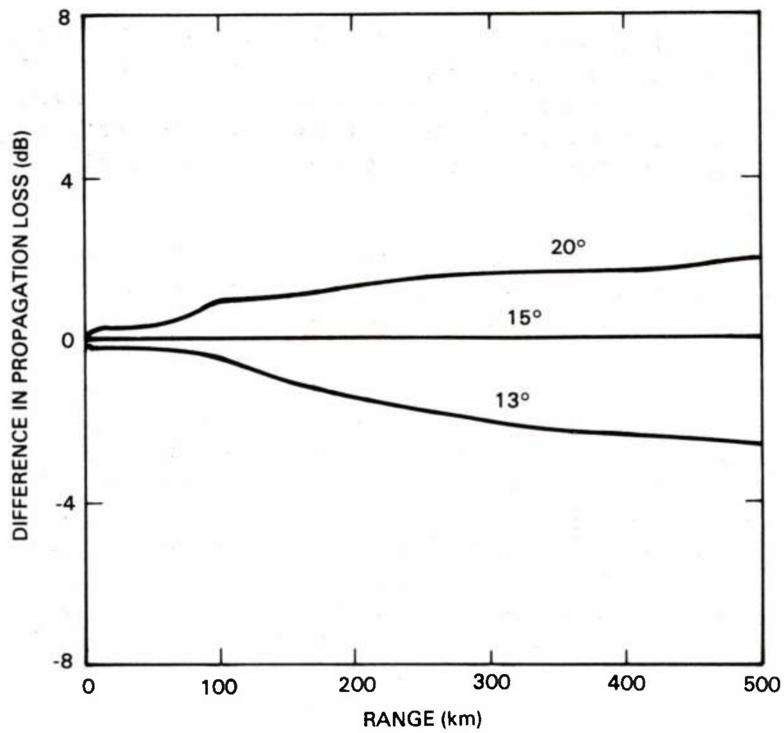

Figure 22. Difference between propagation loss computations with the ice loss curve starting at 13°, 15°, and 20° grazing angle.

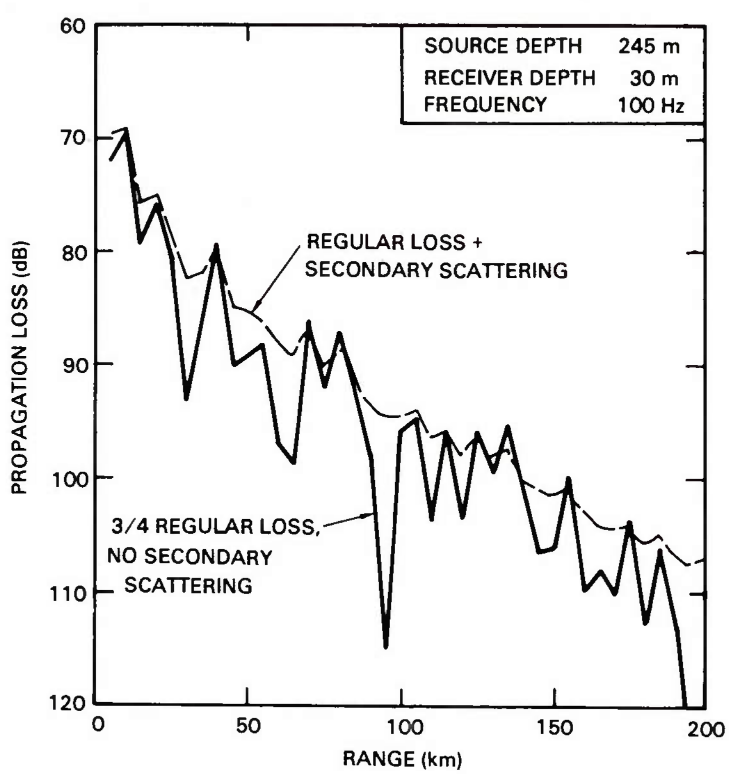

Figure 23. Comparison of propagation losses computed with and without secondary scattering.

table and none in the scattering loss table. The surface scattering integrals therefore make no contribution to the field. The most apparent difference between the two computations in figure 23 is the much greater fluctuation in the losses without secondary scattering. This is because the scattering integrals give a rather smooth loss function that fills in the interference nulls in the coherent mode results.

The source-receiver depth dependence of the computations with and without secondary scattering is complicated. We have not studied it in detail. Here we will point out one difference and show one comparison as an introduction to the topic.

In the Arctic positive gradient sound speed profile, a deep source or receiver fails to intercept some rays which pass above it. If a shallow source is producing such rays, scattering can direct some energy from them down to a deeper receiver. By reciprocity, the same thing can happen for a deep source and shallow receiver. This produces a scattered field that is relatively strong compared to the direct field. Thus, when source and receiver are at different depths, the computation with secondary scattering will show relatively less loss than that without secondary scattering. When source and receiver are near the same depth, this extra advantage is lost and losses computed without secondary scattering are relatively smaller.

The above effect is shown in figure 24. Random phase mode losses are shown for ranges of 100 and 200 km. In general, the losses with secondary scattering are greater when source and receiver are at the same depth and smaller when they are at different depths. The two computations are roughly equal, because of the reduction of the surface loss to 75 percent for the no secondary scatter case.

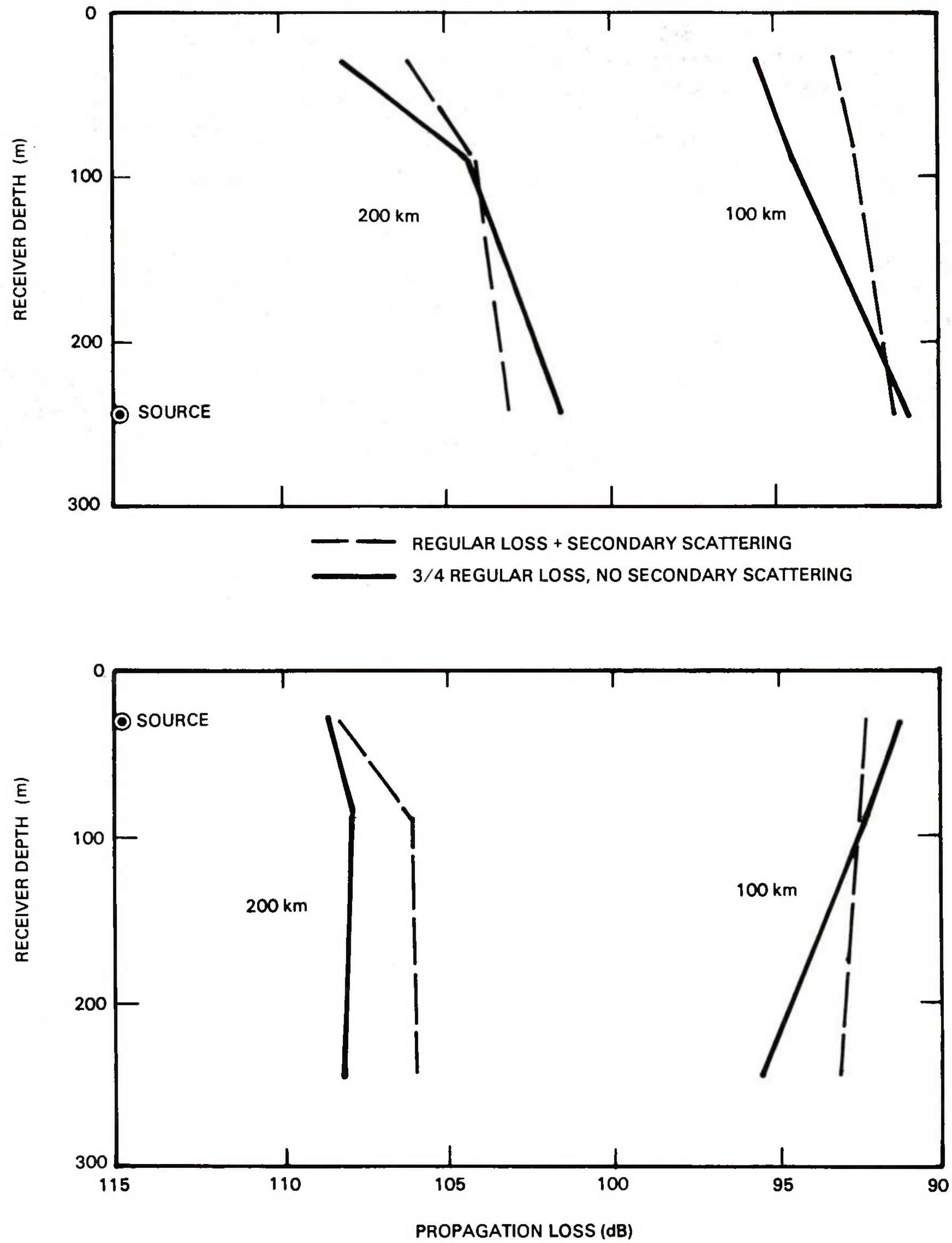

Figure 24. Propagation losses at two ranges and three receiver depths computed with and without secondary scattering.

CONCLUSION

A normal mode computer model has been adapted to Arctic underwater sound propagation. The model integrates over ray paths from the rough surface to the source and receiver to compute the scattered part of the sound field. Ice scattering losses have been determined, and with their use the model gives very good agreement with observed Arctic data. Ice attenuation loss is incorporated in the model, but the data available are not sufficient to determine the small differences in propagation loss caused by ice attenuation.

Available propagation loss data do not permit evaluation of the exact functional dependence of scattering loss upon grazing angle. However, experimental configurations are discussed that would help determine the functional dependence.

It is shown that a program which does not use secondary scattering can obtain results approximating ours if an ice scattering loss of 75 percent of our loss in decibels is used. However, the source receiver dependence of the results cannot be made to coincide exactly.

REFERENCES

1. H.P. Bucker, "Wave Propagation in a Duct with Boundary Scattering (with application to a Surface Duct)," J. Acoust. Soc. Am. 68, 1768-1772 (1976).

2. H.P. Bucker, "Sound Propagation in a Channel with Lossy Boundaries," J. Acoust. Soc. Am. 48, 1187-1194 (1970).

3. O.I. Diachok, "Effects of Sea-Ice Ridges on Sound Propagation in the Arctic Ocean," J. Acoust. Soc. Am. 59, 1110-1120 (1976).

4. R.H. Mellen and H.W. Marsh, "Underwater Sound in the Arctic Ocean," AVCO Marine Electronics Office Report MED-65-1002 (Aug 1965).

5. B.M. Buck, "Preliminary Under Ice Propagation Models Based on Synoptic Ice Roughness," Polar Research Lab TR-30 (May 1981).

6. L.A. LeSchack and D.C. Chang, "Arctic Under-Ice Roughness," Development and Resources Transportation Co. Tech. Rept. (1977).

7. A.R. Milne, "A 90 Km Sound Transmission Test in the Arctic," J. Acoust. Soc. Am. 35, 1459-1461 (1963).

APPENDIX A: SAMPLE RUNS

This appendix gives two sample runs to assist users of the Arctic propagation model in setting up run decks. Figure A-1 is an explanation of input card formats prepared by D. White of NORDA. Following that, two sample runs are presented, each of which consists of an input deck of ten cards and the computer printout which results.

The first of the two runs, entitled "First Sample Run" (fig A-2), is a 100-Hz run using 250 modes. Bottom loss, ice scattering, and ice loss tables are all read in. A five-layer Arctic sound speed profile and two receiver depths are read in. An additional receiver, at the same depth as the source, is always added by the program (if not read in by the user.)

The second sample run, entitled "Second Sample Run" (fig. A-2), is a 200-Hz run and only requests modes up to phase velocity 1510 m/sec. (This is not an adequate number, as one can check by making a run with a larger number of modes and noting the difference in propagation loss.) This run requests standard ice roughness losses for ice depth standard deviation of 2.5 m by placing only this number on the input card for ice scattering loss. The standard winter ice loss is obtained by using zero (a blank) on the ice loss card.

The propagation loss on the printouts is given at lines entitled RKM. The following lines, entitled 10 and 90 percent, give certain expected values resulting from the random phase relation between the coherent and incoherent fields, and are not discussed in this report. The lines entitled Coherent SL give the propagation loss of the coherent or normal mode field only. Finally, for every tenth range, a random phase loss is given, which is equivalent to the loss of a range averaged intensity.

```
C
C************************************************************************
C                    NORMAL MODE PROGRAM FOR REAL EIGEN VALUES
C                         WITH UNDER ICE CAPABILITIES
C                DEVELOPED BY HP BUCKER AND DF GORDON
C                             NAVAL OCEAN SYSTEMS CENTER
C                             SAN DIEGO, CA.
C************************************************************************
C
C!!!!!!!!!!!!!!!!!!!!!!!!!!!!!!!!!!!!!!!!!!!!!!!!!!!!!!!!!!!!!!!!!!!!!!!!
C      ***  INPUT CARD TYPE 0, TITLE OF RUN, ETC.   ***
C FORMAT (7A6,I1,2F8.0,2F6.0,2I1,2I2)
C
C            TITLE  : TITLE OF RUN
C            IPLOT  : =2 GIVES AVERAGE LEVEL AND 10% AND 90% VALUES TO
C                        UNIT 11 [MUST SET I2OS FLAG]
C                     =1 GIVES AVERAGE LEVEL ONLY TO UNIT 11
C                     ELSE NO OUTPUT TO UNIT 11
C            XXXX1  : NOT USED
C            XXXX2  : NOT USED
C            XXXX3  : NOT USED
C            XXXX4  : NOT USED
C            I3DBP  : NON ZERO THEN BEAM RESPONE OUTPUT TO UNIT 12
C            I2OS   : =0 NO SECOND ORDER SCATTERING
C                     ELSE CALCULATE SECOND ORDER SCATTERING
C            IVLA   : NON ZERO THEN DO BEAM PATTERN CALCULATION
C                     [NEEDS SPECIAL RECEIVER DEPTH INPUT, RCD(2)<0]
C            NAVG   : NUMBER OF RANGE POINTS TO AVERAGE FOR LOSS OUTPUT
C
C!!!!!!!!!!!!!!!!!!!!!!!!!!!!!!!!!!!!!!!!!!!!!!!!!!!!!!!!!!!!!!!!!!!!!!!!
C         ***  INPUT CARD TYPE 1, SOURCE PARAMETERS, ETC.   ***
C FORMAT (I4,F8.2,2F6.2,F7.2,F4.2,F5.2,3I3,F4.0)
C
C            NSOR   : NUMBER OF SOURCES FOR SOURCE BEAM PATTERN.
C            SD     : SOURCE DEPTH
C            ASOR   : ELEVATION OF MAIN BEAM [IF NSOR>0]
C            DSOR   : SEPARTION BETWEEN SOURCES.
```

Figure A-1. Input card formats.

```
C              VRATIO : VELOCITY RATIO (SEDIMENT TO WATER) FOR BOTTOM
C                       HALF SPACE [IF NO BOTTOM LOSS TABLE IS READ IN
C                       AND A BOTTOM IS WANTED]
C              DRATIO : DENSITY RATIO (SEDIMENT TO WATER)
C              RLAT   : LATITUDE FOR CURVED EARTH CORRECTION IF NOT ZERO
C                       NO CURVED EARTH CORRECTION IF EQUAL TO ZERO
C              NMODS  : NUMBER OF POINTS FOR MODE DEPTH PLOT
C              NMOD1  : FIRST MODE TO BE PLOTTED
C              NMOD2  : LAST MODE TO BE PLOTTED
C              DMODS  : DISTANCE BETWEEN POINTS FOR MODE PLOT
C
C
C!!!!!!!!!!!!!!!!!!!!!!!!!!!!!!!!!!!!!!!!!!!!!!!!!!!!!!!!!!!!!!!!!!!!!!!
C                   ***  INPUT CARD TYPE 2  ***
C FORMAT (I4,F7.3,F5.3,F8.3,F5.0,3F6.1,2(I2,I1),
C         2I2,2F3.1,2I1,F3.2,F4.1,I2,I2)
C
C              LNM    : MAXIMUM NUMBER OF MODES TO BE USED
C              RFK    : FIRST RANGE [UNITS IN NM OR KM] POINT


C              DRK    : RANGE STEP SIZE
C              RLK    : LAST RANGE POINT
C              FREQ   : FREQUENCY [HZ]
C              PVMIN  : IF NON ZERO, MINIMUM PHASE SPEED OF MODE
C              PVMAX  : IF NON ZERO, MAXIMUM PHASE SPEED OF MODE
C              PVSUR  : IF NON ZERO, PHASE SPEED LIMIT SEARCH FOR
C                       MODES; BEYOND THIS VALUE EXTRAPOLATION IS USED.
C                       MODE NUMBER IS GREATER THAN MSURCH.
C              MSURCH : CORRESPONDING MODE NUMBER TO PVSUR; USED IN
C                       CONJUCTION WITH PVSUR.
C              ISIP   : PRINT DENSITY FOR DEBUG PURPOSES; 1 GENERATES
C                       FULL DEBUG PRINT UP TO 4 WHICH GENERATES LITTLE
C                       DEBUG PRINT
C              IXXXX  : NOT USED
C              IATTEN : VOLUMN ATTENUATION FLAG; =0 NO VOLUMN ATTENUATION.
C                       NOT EQUAL TO ZERO THORP'S VOLUMN ATTENUATION
C              IRG    : ROUGH SURFACE FLAG; =0 NO ROUGH SURFACE
C                                          <>0 ROUGH SURFACE
C              IICE   : ICE LOSS FLAG; =<0 NO LOSS INTO ICE
```

Figure A-1. (Continued)

```
C                                           >0 LOSS INTO ICE, EXTERNAL
C                                             INPUT.
C             WVHT   : WAVE HEIGHT; ONE THIRD SIGNIFICANT.
C             WIND   : WIND SPEED IN KTS [FOR WAVE HEIGHT CONVERSION]
C             IBOTL  : EXTERNAL BOTTOM LOSS TABLE FLAG; =0 NO EXTERNAL
C                      BOTTOM LOSS TABLE READ, <>0 READ BOTTOM LOSS TABLE
C             IXXX   : NOT USED
C             RICE   : ICE ROUGHNESS PARAMETER; .LE. 0.0 SURFACE LOSS
C                      TABLE FROM OTHER MEANS, E.G. WAVE HEIGTH, ELSE
C                      STANDARD TABLE USED AND MULTIPLIED BY RICE. THAT
C                      IS, RICE=1 IS THE STANDARD TABLE DEVELOPED BY
C                      DAVE GORDON AS A FIT TO DATA. SEE 'MODEL FOR
C                      ARCTIC PROPAGATION LOSS USING SCATTERING INTEGRALS
C                      AND EMPIRICAL REFLECTION LOSSES', DF GORDON AND
C                      HP BUCKER; PAPER M11 107TH MEETING OF THE ACOUS.
C                      SOCIETY OF AMERICA, MAY 1984.
C             SORLEV : SOURCE LEVEL IN DB; IF ZERO TRANSMISSION LOSS IS.
C                      OUTPUT, IF NOT ZERO THE RECEIVED LEVEL IS OUTPUT
C             ILASVX : MAXIMUM NUMBER OF TIMES MODE SEARCH WILL ITERATE
C                      TO FIND A MODE [DEFAULT IS 10]
C             INAUTM : RANGE UNIT FLAG; =0 RANGE IS KM
C                                       <>0 RANGE IS NM
C
C
C!!!!!!!!!!!!!!!!!!!!!!!!!!!!!!!!!!!!!!!!!!!!!!!!!!!!!!!!!!!!!!!!!!!!!!!!!!!
C         ***  INPUT CARD TYPE 2A, BOTTOM LOSS TABLE  ***
C              (ONLY IF IBOTL IS NOT EQUAL TO ZERO)
C FORMAT (20F4.2)
C
C             BOTLT  : BOTTOM LOSS VALUES (DB); STARTS AT ZERO DEGREES
C                      GOES TO 90 DEGREES IN STEPS OF ONE DEGREE.
C                      NOTE, IF MORE THAN FIVE VALUES ARE READ IN AND A
C                            ZERO VALUE IF THEN READ IN, THE REMAINING
C                            TABLEIS FILLED WITH THE LAST NON ZERO VALUE.
C
C
```

Figure A-1. (Continued)

```
C!!!!!!!!!!!!!!!!!!!!!!!!!!!!!!!!!!!!!!!!!!!!!!!!!!!!!!!!!!!!!!!!!!!!!!!!
C      ***  INPUT CARD TYPE 2B, SURFACE LOSS DUE TO ROUGHNESS  ***
C               (ONLY IF IRG IS NOT EQUAL TO ZERO)
C FORMAT (11(F3.0,F4.1))
C
C             AN      : ANGLE AT SURFACE
C                       NOTE, IF AN(2)<=0, THEN AN(1)[ >0.0001 OR DEFAULT
C                       TO 2] IS THE VALUE OF THE ICE STANDARD DEVIATION
C                       ROUGHNESS, AND A STANDARD LOSS TABLE IS GENERATED.
C                       SEE ABOVE REF.
C             SL      : LOSS AT SURFACE [DB]
C
C!!!!!!!!!!!!!!!!!!!!!!!!!!!!!!!!!!!!!!!!!!!!!!!!!!!!!!!!!!!!!!!!!!!!!!!!
C     ***  INPUT CARD TYPE 2C, SURFACE LOSS DUE TO ICE ABSORPTION  ***
C                (ONLY IF IICE IS NOT EQUAL TO ZERO)
C FORMAT (11(F3.0,F4.1))
C
C             AN      : ANGLE(DEGREES) AT THE SURFACE. IF AN(2).LE.0. THEN
C                       IF AN(1).LT. 0 A STANDARD SUMMER VALUE TABLE IS
C                                       GENERATED
C                       ELSE            A STANDARD WINTER VALUE TABLE IS
C                                       GENERATED
C             SL      : LOSS AT SURFACE [DB]
C
C!!!!!!!!!!!!!!!!!!!!!!!!!!!!!!!!!!!!!!!!!!!!!!!!!!!!!!!!!!!!!!!!!!!!!!!!
C          ***  INPUT CARD TYPE 3, SOUND SPEED PROFILE  ***
C FORMAT (5(F8.1,F8.2))
C
C             ZWL     : DEPTH (M).  READ UNTIL ZWL(I)=0 FOR I>1.
C             VWL     : SOUND SPEED (M/S)
C
C!!!!!!!!!!!!!!!!!!!!!!!!!!!!!!!!!!!!!!!!!!!!!!!!!!!!!!!!!!!!!!!!!!!!!!!!
C           ***  INPUT CARD TYPE 4, RECEIVER DEPTHS    ***
C FORMAT (10F8.2)
C
C             RCD     : RECEIVER DEPTH (M). READ UNTIL RDC(I)=0, I>1.
C                       NOTE. IF RCD(2) IS .LT.0 THEN THE NUMBER OF
C                       RECEIVER DEPTHS IS LNR [=-RCD(2)], RCD(3) IS
C                       INCREMENTAL SPACING AND RCD(1) IS THE TOP OF
C                       THE STRING OF RECEIVERS.
C
```

Figure A-1. (Continued)

```
C!!!!!!!!!!!!!!!!!!!!!!!!!!!!!!!!!!!!!!!!!!!!!!!!!!!!!!!!!!!!!!!!!!!!!!
C                    ***  INPUT ARRAY PARAMETERS  ***
C                   (ONLY IF IVLA IS NOT EQUAL TO ZERO)
C FORMAT (I5,2F5.1,F5.2)
C
C             NAL    : NUMBER OF BEAMS
C             PHI1   : ANGLE OF THE FIRST BEAM
C             DPH1   : INCREMENTAL ANGLE FOR BEAMS
```

Figure A-1. (Continued)

```
00        INPUT DECK
00     12345678901234567890123456789012345678901234567890123456789012345678901234567890
00
00
00     --------------------------------------------------------------------------------
00            SAMPLE RUN                            1                             2
00            245
00      250  10      10.  200      100 1435              4  1 11       10
00     0     6  14   18  195 202 208 213 227 252 3
00            20.3.3890.3.38
00            15.     17. 2. 90. 2.
00             1435.   300.     1454.6  500.     1459.6  1200.    1468.2  2000.    1482.7
00     3500.   1507.
00       30.     90.
00
00     --------------------------------------------------------------------------------
00
00
00     12345678901234567890123456789012345678901234567890123456789012345678901234567890
```

Figure A-2. First sample run.

```
***  REM2., ARCTIC PROPAGATION PROGRAM  ***  .

     SAMPLE RUN

   IPLOT      XXXX1      XXXX2      XXXX3      XXXX4   I 3D BP   I 2 OS   I VLA    N AVG
     1          0.         0.         0.         0.        0        2        0        0

***  CARD TYPE 1, SOURCE PARAMETERS, ETC.  ***

    NSOR      SD     A SDR      DSDR     VRATIO    DRATIO     RLAT     NMODS    NMOD1    NMOD2    DMODS
      0    245.00     .00        .00       .00      1.50       .00       0        0        0       .0

INPUT CARD TYPE 2, RANGE LIMITS ARE KM  **

   LNM       RFK        DRK          RLK       FREQ      PVMIN      PVMAX      PVSUR  MSURCH
   250     10.000     10.000      200.000     100.0    1435.00       .00        .00      3

  I SIP   I XXXX   IATTEN    I RG   I ICE  S.WVHT WIND(KNT)  I BOT LOS  I XXX  ICE RATIO  SOR LEV   ILASV   INAUTM
    4        0        1        1     10     .00      .00         1        0       .00       .0        0        0

***  READ IN BOTTOM LOSS TABLE, CARD TYPE 2A  ***

BOT LOS(DB)       .00      .60      1.40     1.80     1.95     2.02     2.08     2.13     2.27     2.52
                 3.00      .00       .00      .00      .00      .00      .00      .00      .00      .00

**  INPUT 2B, SURFACE LOSS DUE TO ROUGHNESS  **

    0.      .0        20.     3.4       90.     3.4        0.     .0        0.     .0
    0.      .0         0.      .0        0.      .0        0.     .0        0.     .0        0.     .0

**  INPUT 2C, SURFACE LOSS DUE TO ICE ABSORPTION  **

    0.      .0        15.      .0       17.     2.0       90.    2.0        0.     .0
    0.      .0         0.      .0        0.      .0        0.     .0        0.     .0        0.     .0

SURFACE LOSS TABLE
     GZS        RG LOSS      RG2 LOSS    ICE ABSORB    TOTAL LOSS      SCATF
      0           .000          .000         .000          .000       .000000
      1           .000          .169         .000          .169       .038166
      2           .000          .338         .000          .338       .074876
      3           .000          .507         .000          .507       .110184
      4           .000          .676         .000          .676       .144145
      5           .000          .845         .000          .845       .176810
      6           .000         1.014         .000         1.014       .208228
      7           .000         1.183         .000         1.183       .238447
      8           .000         1.352         .000         1.352       .267513
      9           .000         1.521         .000         1.521       .295469
     10           .000         1.690         .000         1.690       .322358
     11           .000         1.859         .000         1.859       .348222
     12           .000         2.028         .000         2.028       .373098
     13           .000         2.197         .000         2.197       .397024
```

Figure A-2. (Continued)

```
     14          .000        2.366        .000        2.366       .420037
     15          .000        2.535        .000        2.535       .442172
     16          .000        2.704       1.000        3.704       .463463
     17          .000        2.873       2.000        4.873       .483940
     18          .000        3.042       2.000        5.042       .503636
     19          .000        3.211       2.000        5.211       .522581
     20          .000        3.380       2.000        5.380       .540802

VOL. ATTEN. =    .00 DB/KM AT    100. HZ **

***  INPUT CARD TYPE 3, SOUND SPEED PROFILE  ***

(Z, V)          .0   1435.00      300.0   1454.60      500.0   1459.60     1200.0   1468.20     2000.0   1482.70

***  INPUT CARD TYPE 3, SOUND SPEED PROFILE  ***

(Z, V)     3500.0   1507.00         .0       .00         .0       .00         .0       .00         .0       .00

***  BOT LOSS TABLE (IN DB), ANGLES FROM 0 TO 29 DEG  **

      .00       .60      1.40      1.80      1.95      2.02      2.08      2.13      2.27      2.52
     3.00      3.00      3.00      3.00      3.00      3.00      3.00      3.00      3.00      3.00
     3.00      3.00      3.00      3.00      3.00      3.00      3.00      3.00      3.00      3.00

***  PARAMETER CHECK  ***
     NWL    INMINV       VMIN    INMAXV       VMAX      PVMIN      PVMAX       VBOT      VBSED      VMAX2
      5         1     1435.00        6     1507.00    1435.00    2870.00    1507.00    1657.70    1507.00

 ***  INPUT CARD TYPE 4, RECEIVER DEPTHS  ***
     30.00      90.00        .00       .00       .00       .00       .00       .00       .00       .00

***  N.B.. RCV. MUST BE ADDED WITH RCD(LNR) = S  FOR CALCULATION OF SCATTERED FIELD  ***


***  SOUND SPEED PROFILE  ***

    DEPTH      SPEED       NL      SD      RCD                   SPEED VS. DEPTH
       .0    1435.00        1                          1
     30.0    1436.92        0               +           1
     90.0    1440.80        0               +             1
    245.0    1450.95        0       *       +                  1
    300.0    1454.60        2                                   1
    500.0    1459.60        3                                     1
   1200.0    1468.20        4                                         1
   2000.0    1482.70        5                                                1
   3500.0    1507.00        6                                                           1

 ***  BEGIN SEARCH FOR MODES  ***
* MODE   1   0   1   4    1440.845       .217       5.16        .00        .00        .87       4018.
```

Figure A-2. (Continued)

** CK. DOUBLE DUCT				1	1442.2704	1442.5530	1442.5544	1442.5537	.3436+00	.3400-05	.3409-05	.3405-05
** CK. DOUBLE DUCT				2	1442.2704	1442.5530	1442.5537	1442.5533	.3436+00	.3400-05	.3405-05	.3402-05
** CK. DOUBLE DUCT				3	1442.2704	1442.5530	1442.5533	1442.5532	.3436+00	.3400-05	.3402-05	.3401-05
** CK. DOUBLE DUCT				4	1442.2704	1442.5530	1442.5532	1442.5531	.3436+00	.3400-05	.3401-05	.3401-05
** CK. DOUBLE DUCT				5	1442.2704	1442.5530	1442.5531	1442.5530	.3436+00	.3400-05	.3401-05	.3400-05
* MODE	2	0	2	5	1445.266	.218	6.83	.00	.00	1.15	5296.	
* MODE	3	0	2	6	1448.916	.219	7.95	.00	.00	1.34	6139.	
* MODE	4	0	2	5	1452.159	.219	8.82	2.34	.00	1.49	6790.	
* MODE	5	0	3	5	1455.023	.177	9.52	4.29	.00	1.61	9077.	
* MODE	6	0	3	4	1457.076	.142	9.99	5.26	.00	1.69	11922.	
* MODE	7	0	3	5	1458.734	.130	10.35	5.92	.00	1.75	13425.	
* MODE	8	0	3	4	1460.154	.100	10.65	6.44	.00	1.80	17912.	
* MODE	9	0	3	4	1461.248	.087	10.68	6.81	.00	1.84	21122.	
* MODE	10	0	3	4	1462.218	.080	11.07	7.12	.00	1.87	23263.	
* MODE	11	0	3	3	1463.098	.076	11.25	7.39	.00	1.90	24939.	
* MODE	12	0	3	4	1463.935	.073	11.41	7.64	.00	1.93	26382.	
* MODE	13	0	4	4	1464.727	.071	11.56	7.87	.00	1.95	27645.	
* MODE	14	0	4	3	1465.483	.069	11.71	8.08	.00	1.98	28777.	
* MODE	15	0	4	3	1466.216	.067	11.84	8.28	.00	2.00	29816.	
* MODE	16	0	4	3	1466.929	.066	11.98	8.47	.00	2.02	30781.	
* MODE	17	0	4	3	1467.621	.065	12.10	8.65	.00	2.05	31680.	
* MODE	18	0	4	3	1468.300	.065	12.23	8.82	.00	2.07	31683.	
* MODE	19	0	4	3	1468.981	.067	12.35	8.99	.00	2.09	30990.	
* MODE	20	0	4	3	1469.675	.068	12.47	9.16	.00	2.11	30920.	
* MODE	21	0	4	3	1470.379	.069	12.59	9.33	.00	2.13	31023.	
* MODE	22	0	4	3	1471.074	.069	12.71	9.49	.00	2.15	31207.	
* MODE	23	0	4	3	1471.762	.069	12.83	9.65	.00	2.17	31435.	
* MODE	24	0	4	3	1472.450	.069	12.95	9.80	.00	2.19	31693.	
* MODE	25	0	4	3	1473.131	.069	13.06	9.96	.00	2.21	31967.	
* MODE	26	0	4	3	1473.808	.069	13.18	10.10	.00	2.23	32252.	
* MODE	27	0	4	3	1474.480	.069	13.29	10.25	.00	2.25	32544.	
* MODE	28	0	4	3	1475.145	.069	13.40	10.39	.00	2.26	32838.	
* MODE	29	0	4	3	1475.805	.069	13.50	10.53	.00	2.28	33134.	
* MODE	30	0	4	3	1476.459	.069	13.61	10.67	.00	2.30	33429.	
* MODE	31	0	4	3	1477.109	.069	13.71	10.80	.00	2.32	33723.	
* MODE	32	0	5	3	1477.753	.069	13.82	10.93	.00	2.33	34015.	
* MODE	33	0	5	3	1478.393	.069	13.92	11.06	.00	2.35	34305.	
* MODE	34	0	5	3	1479.027	.068	14.02	11.18	.00	2.37	34592.	
* MODE	35	0	5	3	1479.657	.068	14.11	11.31	.00	2.38	34876.	
* MODE	36	0	5	3	1480.282	.068	14.21	11.43	.00	2.40	35156.	
* MODE	37	0	5	3	1480.903	.068	14.30	11.54	.00	2.42	35433.	
* MODE	38	0	5	3	1481.520	.068	14.40	11.66	.00	2.43	35708.	
* MODE	39	0	5	3	1482.133	.068	14.49	11.77	.00	2.45	35978.	
* MODE	40	0	5	3	1482.739	.068	14.58	11.89	.00	2.46	36435.	
* MODE	41	0	5	2	1483.338	.066	14.67	12.00	.00	2.48	37277.	
* MODE	42	0	5	3	1483.926	.066	14.75	12.10	.00	2.49	37829.	
* MODE	43	0	5	2	1484.503	.065	14.84	12.21	.00	2.51	38304.	
* MODE	44	0	5	3	1485.074	.065	14.92	12.31	.00	2.52	38738.	
* MODE	45	0	5	3	1485.641	.065	15.00	12.41	.00	2.54	39145.	
* MODE	46	0	5	3	1486.203	.067	15.08	12.50	.00	2.63	39531.	
* MODE	47	0	5	2	1486.758	.068	15.16	12.60	.00	2.73	39900.	
* MODE	48	0	5	3	1487.310	.070	15.24	12.70	.00	2.82	40256.	

Figure A-2. (Continued)

* MODE	49	0	5	2	1487.858	.072	15.32	12.79	.00	2.91	40599.
* MODE	50	0	5	2	1488.401	.073	15.39	12.88	.00	3.00	40932.
* MODE	55	0	5	2	1491.061	.081	15.76	13.32	.00	3.42	42474.
* MODE	60	0	5	2	1493.640	.087	16.11	13.73	.00	3.83	43663.
* MODE	65	0	5	2	1496.151	.093	16.44	14.12	.00	4.22	45138.
* MODE	70	0	5	2	1498.602	.099	16.75	14.49	.00	4.58	46323.
* MODE	75	0	5	2	1501.001	.103	17.05	14.84	.00	4.88	47433.
* MODE	80	0	6	3	1503.354	.102	17.34	15.17	.00	4.93	48480.
* MODE	85	0	6	3	1505.672	.101	17.62	15.49	.00	4.98	49474.
* MODE	90	0	6	3	1508.123	.150	17.92	15.83	2.21	6.51	43488.
* MODE	95	0	6	3	1510.910	.182	18.24	16.20	4.12	7.04	38581.
* MODE	100	0	6	3	1513.995	.203	18.59	16.59	5.51	7.19	35434.
* MODE	105	0	6	3	1517.343	.222	18.96	17.01	6.69	7.32	33001.
* MODE	110	0	6	3	1520.939	.242	19.35	17.45	7.76	7.51	30990.
* MODE	115	0	6	3	1524.778	.266	19.76	17.90	8.76	7.80	29267.
* MODE	120	0	6	3	1528.855	.297	20.18	18.37	9.70	8.24	27757.
* MODE	125	0	6	2	1533.171	.317	20.61	18.85	10.60	8.38	26413.
* MODE	130	0	6	2	1537.727	.333	21.06	19.34	11.47	8.38	25202.
* MODE	135	0	6	2	1542.527	.348	21.52	19.84	12.32	8.38	24101.
* MODE	140	0	6	2	1547.573	.363	21.99	20.35	13.15	8.38	23092.
* MODE	145	0	6	2	1552.871	.378	22.47	20.87	13.96	8.38	22163.
* MODE	150	0	6	2	1558.426	.393	22.96	21.40	14.76	8.38	21303.
* MODE	155	0	6	2	1564.244	.409	23.45	21.94	15.55	8.38	20502.
* MODE	160	0	6	2	1570.332	.424	23.96	22.49	16.33	8.38	19755.
* MODE	165	0	6	2	1576.697	.440	24.48	23.04	17.10	8.38	19055.
* MODE	170	0	6	2	1583.348	.456	25.00	23.60	17.87	8.38	18397.
* MODE	175	0	6	2	1590.293	.471	25.53	24.16	18.63	8.38	17776.
* MODE	180	0	6	2	1597.541	.487	26.07	24.74	19.38	8.38	17190.
* MODE	185	0	6	2	1605.104	.504	26.62	25.32	20.14	8.38	16635.
* MODE	190	0	6	2	1612.990	.520	27.17	25.90	20.89	8.38	16109.
* MODE	195	0	6	2	1621.213	.537	27.73	26.49	21.64	8.38	15608.
* MODE	200	0	6	2	1629.783	.554	28.30	27.09	22.38	8.38	15131.
* MODE	210	0	6	2	1648.012	.588	29.45	28.31	23.87	8.38	14241.
* MODE	220	0	6	2	1667.793	.624	30.64	29.54	25.37	8.38	13426.
* MODE	230	0	6	2	1689.400	.661	31.85	30.81	26.87	8.38	12670.
* MODE	240	0	6	2	1712.903	.700	33.10	32.11	28.38	8.38	11970.
* MODE	250	0	6	2	1738.492	.740	34.37	33.43	29.91	8.38	11317.

Figure A-2. (Continued)

SOUND LEVEL, RCV AT		30.0	90.0	245.0								
	RANGE	SL	SL	SL	SL	SL	SL	SL	SL	SL	SL	SL
RKM	10.000	68.9	71.8	72.9								
10 PER-CENT		74.0	78.4	79.3								
90 PER-CENT		66.4	68.9	70.1								
COHERENT SL		69.8	73.5	74.5								
RANDOM	10.000	71.5	72.5	69.9								
RKM	10.000	68.9	71.8	72.9								
RKM	20.000	74.9	78.2	76.2								
10 PER-CENT		81.8	87.9	82.5								
90 PER-CENT		72.0	74.7	73.4								
COHERENT SL		76.7	82.6	77.7								
RKM	30.000	82.2	81.4	81.7								
10 PER-CENT		92.6	91.4	90.9								
90 PER-CENT		78.7	77.9	78.3								
COHERENT SL		96.4	86.5	85.2								
RKM	40.000	79.4	85.1	82.1								
10 PER-CENT		85.8	95.3	89.2								
90 PER-CENT		76.5	81.6	79.1								
COHERENT SL		81.0	96.1	84.1								
RKM	50.000	85.1	83.2	83.8								
10 PER-CENT		95.3	91.3	91.4								
90 PER-CENT		81.5	80.1	80.7								
COHERENT SL		91.6	85.9	86.1								
RKM	60.000	87.7	86.0	83.9								
10 PER-CENT		98.1	94.9	90.0								
90 PER-CENT		84.2	82.7	81.1								
COHERENT SL		97.1	89.3	85.3								
RKM	70.000	86.5	90.0	89.4								
10 PER-CENT		94.2	100.3	99.3								
90 PER-CENT		83.4	86.5	86.0								
COHERENT SL		88.9	99.0	94.1								

Figure A-2. (Continued)

RKM	80.000	87.7	90.5	89.2
10 PER-CENT		95.1	100.3	96.8
90 PER-CENT		84.7	87.1	86.1
COHERENT SL		89.9	95.0	91.5
RKM	90.000	92.8	92.1	91.0
10 PER-CENT		103.1	102.1	99.2
90 PER-CENT		89.2	88.6	87.9
COHERENT SL		100.7	97.5	93.7
RKM	100.000	93.7	92.2	94.0
10 PER-CENT		104.1	101.6	104.2
90 PER-CENT		30.2	88.8	90.4
COHERENT SL		101.8	95.9	100.8
RANDOM	100.000	93.2	92.5	91.3
RKM	100.000	93.7	92.2	94.0
RKM	110.000	95.9	95.5	93.0
10 PER-CENT		106.1	105.8	101.1
90 PER-CENT		92.4	92.0	89.8
COHERENT SL		107.3	104.2	95.6
RKM	120.000	97.1	97.6	97.5
10 PER-CENT		107.4	108.0	107.7
90 PER-CENT		93.5	94.1	93.9
COHERENT SL		109.9	124.8	108.2
RKM	130.000	97.2	95.7	98.2
10 PER-CENT		107.2	104.5	108.6
90 PER-CENT		93.8	92.4	94.7
COHERENT SL		102.3	98.9	105.6
RKM	140.000	99.0	99.1	96.4
10 PER-CENT		109.3	109.4	104.5
90 PER-CENT		95.5	95.5	93.3
COHERENT SL		106.1	108.5	99.1
RKM	150.000	100.9	100.1	97.1
10 PER-CENT		111.2	110.4	104.5
90 PER-CENT		97.3	96.6	94.0

Figure A-2. (Continued)

```
   COHERENT SL          109.5     107.5      99.2

  RKM       160.000     101.8      99.3     100.8

  10 PER-CENT           112.1     107.9     110.9
  90 PER-CENT            98.2      96.0      97.3

   COHERENT SL          109.9     102.3     106.1

  RKM       170.000     103.3     100.7      99.7

  10 PER-CENT           113.6     110.0     107.4
  90 PER-CENT            99.8      97.4      96.6

   COHERENT SL          112.6     104.4     102.1

  RKM       180.000     105.0     103.7     102.9

  10 PER-CENT           115.3     114.1     112.8
  90 PER-CENT           101.4     100.2      99.5

   COHERENT SL          119.2     112.6     107.9

  RKM       190.000     105.6     104.7     102.2

  10 PER-CENT           115.8     115.0     110.4
  90 PER-CENT           102.0     101.2      99.0

   COHERENT SL          117.2     113.0     104.9

  RKM       200.000     106.2     105.8     105.7

  10 PER-CENT           116.5     116.2     116.1
  90 PER-CENT           102.6     102.3     102.2

   COHERENT SL          113.5     114.3     113.7


 RANDOM     200.000     106.0     104.1     103.0

  RKM       200.000     106.2     105.8     105.7
DATA IGNORED - IN CONTROL MODE

$FIN
```

Figure A-2. (Continued)

```
00     INPUT DECK
00    1234567890123456789012345678901234567890123456789012345678901234567890123456789012345678901234567890
00
00
00    --------------------------------------------------------------------------------
00           SAMPLE TWO                                                               2
00           100
00     200 100   20      300      200 1435   1510         4  1  11        10
00        1.4 2.5 3.  3.2 3.4 3.6 4.
00    2.5
00
00            1435.   300.     1454.6  500.     1459.6  1200.    1468.2  2000.    1482.7
00    3500.   1507.
00      10.     50.    200.     400.
00
00    --------------------------------------------------------------------------------
00
00
00    1234567890123456789012345678901234567890123456789012345678901234567890123456789012345678901234567890
```

Figure A-3. Second sample run.

```
***  REM2., ARCTIC PROPAGATION PROGRAM  ***

   SAMPLE TWO

  IPLOT       XXXX1       XXXX2       XXXX3       XXXX4   I 3D BP   I 2 OS   I VLA    N AVG
      0          0.          0.          0.          0.         0        2       0        0

***  CARD TYPE 1, SOURCE PARAMETERS, ETC.  ***

   NSDR        SO     A SOR      OSOR    VRATIO    DRATIO      RLAT     NMODS     NMDD1     NMOD2     OMODS
      0    100.00       .00       .00       .00      1.50       .00         0         0         0        .0

INPUT CARD TYPE 2, RANGE LIMITS ARE KM  **

   LNM        RFK         ORK          RLK        FREQ      PVMIN       PVMAX       PVSUR  MSURCH
   200    100.000      20.000      300.000       200.0    1435.00     1510.00         .00       3

  I SIP    I XXXX   IATTEN      I RG    I ICE  S.WVHT WIND(KNT)   I BOT LOS   I XXX  ICE RATIO  SOR LEV    ILASV    INAUTM
      4         0        1         1       10     .00       .00           1       0        .00       .0        0         0

***  READ IN BOTTOM LOSS TABLE, CARD TYPE 2A  ***

BOT LOS(DB)       .00      1.40      2.50      3.00      3.20      3.40      3.60      4.00       .00       .00
                  .00       .00       .00       .00       .00       .00       .00       .00       .00       .00

**  INPUT 2B, SURFACE LOSS DUE TO ROUGHNESS  **

    3.      .0      0.     .0      0.     .0      0.     .0      0.     .0
    0.      .0      0.     .0      0.     .0      0.     .0      0.     .0      0.     .0
**  STANDARD DEVIATION OF ICE DEPTH IS  2.50 M, (FROM IMPLICIT ICE SCATTERING TABLES)  **

**  INPUT 2C, SURFACE LOSS DUE TO ICE ABSORPTION  **

    0.      .0      0.     .0      0.     .0      0.     .0      0.     .0
    0.      .0      0.     .0      0.     .0      0.     .0      0.     .0      0.     .0
**  IMPLICIT ICE ABSORPTION TABLES USED FOR WINTER  *

SURFACE LOSS TABLE
   GZS         RG LOSS      RG2 LOSS    ICE ABSORB    TOTAL LOSS        SCATF
     0            .000          .000          .000          .000      .000000
     1            .000          .422          .000          .422      .092571
     2            .000          .844          .000          .844      .176573
     3            .000         1.266          .000         1.266      .252799
     4            .000         1.687          .000         1.687      .321968
     5            .000         2.109          .000         2.109      .384735
     6            .000         2.531          .000         2.531      .441691
     7            .000         2.953          .000         2.953      .493374
     8            .000         3.375          .000         3.375      .540273
     9            .000         3.797          .000         3.797      .582831
```

Figure A-3. (Continued)

```
   10        .000        4.219        .000        4.219       .621448
   11        .000        4.641        .000        4.641       .656492
   12        .000        5.062        .000        5.062       .688291
   13        .000        5.484        .000        5.484       .717146
   14        .000        5.906        .000        5.906       .743330
   15        .000        6.328        .000        6.328       .767090
   16        .000        6.750       1.000        7.750       .788651
   17        .000        7.172       2.000        9.172       .808216
   18        .000        7.594       2.000        9.594       .825970
   19        .000        8.016       2.000       10.016       .842080
   20        .000        8.438       2.000       10.437       .856699

VOL. ATTEN. =   .00 DB/KM AT   200. HZ **

***  INPUT CARD TYPE 3, SOUND SPEED PROFILE  ***

(Z, V)         .0    1435.00      300.0   1454.60      500.0   1459.60     1200.0   1468.20     2000.0   1482.70

***  INPUT CARD TYPE 3, SOUND SPEED PROFILE  ***

(Z, V)     3500.0    1507.00         .0       .00         .0       .00         .0       .00         .0       .00

***  BOT LOSS TABLE (IN DB), ANGLES FROM 0 TO 29 DEG  **

      .00      1.40      2.50      3.00      3.20      3.40      3.60      4.00      4.00      4.00
     4.00      4.00      4.00      4.00      4.00      4.00      4.00      4.00      4.00      4.00
     4.00      4.00      4.00      4.00      4.00      4.00      4.00      4.00      4.00      4.00

***  PARAMETER CHECK  ***
     NWL   INMINV      VMIN   INMAXV      VMAX     PVMIN     PVMAX      VBOT     VBSED     VMAX2
      5       1     1435.00      6     1507.00   1435.00   1510.00   1507.00   1657.70   1507.00

 ***  INPUT CARD TYPE 4, RECEIVER DEPTHS  ***
      10.00      50.00     200.00     400.00       .00       .00       .00       .00       .00       .00

***  N.B.., RCV. MUST BE ADDED WITH RCD(LNR) = S  FOR CALCULATION OF SCATTERED FIELD  ***


***  SOUND SPEED PROFILE  ***

     DEPTH      SPEED       NL       SD       RCD                 SPEED VS. DEPTH
        .0     1435.00       1                               1
      10.0     1435.64       0                 +             1
      50.0     1438.21       0                 +               1
     100.0     1441.45       0        *                          1
     200.0     1447.98       0                 +                    1
     300.0     1454.60       2                                          1
     400.0     1457.09       0                 +                          1
     100.0     1441.45       0                 +                 1
     500.0     1459.60       3                                               1
```

Figure A-3. (Continued)

```
  1200.0     1468.20      4                                                      1
  2000.0     1482.70      5                                                             1
  3500.0     1507.00      6                                                                      1

***  BEGIN SEARCH FOR MODES   ***
* MODE   1   0   1   4     1438.674       .541     4.10      .00      .00     1.73     3194.
* MODE   2   0   1  10     1441.442       .542     5.42      .00      .00     2.29     4215.
* MODE   3   0   1   4     1443.720       .544     6.30     3.22      .00     2.66     4890.
* MODE   4   0   1   4     1445.742       .545     6.99     4.42      .00     2.95     5414.
* MODE   5   0   2   4     1447.598       .545     7.56     5.28      .00     3.19     5850.
* MODE   6   0   2   4     1449.334       .546     8.06     5.98      .00     3.40     6227.
* MODE   7   0   2   4     1450.978       .547     8.51     6.57      .00     3.59     6562.
* MODE   8   0   2   4     1452.546       .548     8.91     7.09      .00     3.76     6863.
* MODE   9   0   2   4     1454.038       .549     9.28     7.55      .00     3.92     7136.
* MODE  10   0   2   4     1455.366       .415     9.60     7.93      .00     4.05     9748.
* MODE  11   0   3   5     1456.361       .372     9.83     8.21      .00     4.15    11139.
* MODE  12   0   3   3     1457.282       .349    10.03     8.45      .00     4.23    12130.
* MODE  13   0   3   4     1458.117       .334    10.22     8.67      .00     4.31    12904.
* MODE  14   0   3   4     1458.926       .323    10.39     8.88      .00     4.38    13580.
* MODE  15   0   3   3     1459.674       .289    10.55     9.06      .00     4.45    15405.
* MODE  16   0   3   4     1460.317       .244    10.68     9.22      .00     4.51    18493.
* MODE  17   0   3   3     1460.854       .226    10.80     9.35      .00     4.55    20112.
* MODE  18   0   3   4     1461.377       .215    10.90     9.47      .00     4.60    21431.
* MODE  19   0   3   3     1461.859       .206    11.00     9.59      .00     4.64    22514.
* MODE  20   0   3   2     1462.324       .199    11.09     9.69      .00     4.68    23477.
* MODE  21   0   3   3     1462.771       .194    11.18     9.80      .00     4.72    24339.
* MODE  22   0   3   3     1463.202       .189    11.27     9.89      .00     4.75    25126.
* MODE  23   0   3   3     1463.623       .185    11.35     9.99      .00     4.79    25860.
* MODE  24   0   3   3     1464.033       .182    11.43    10.08      .00     4.82    26543.
* MODE  25   0   3   3     1464.431       .179    11.51    10.16      .00     4.85    27184.
* MODE  26   0   3   3     1464.822       .176    11.58    10.25      .00     4.89    27790.
* MODE  27   0   3   2     1465.204       .173    11.65    10.33      .00     4.92    28366.
* MODE  28   0   3   2     1465.578       .171    11.72    10.41      .00     4.95    28914.
* MODE  29   0   4   3     1465.946       .169    11.79    10.49      .00     4.98    29438.
* MODE  30   0   4   3     1466.308       .167    11.86    10.57      .00     5.00    29943.
* MODE  31   0   4   3     1466.665       .165    11.93    10.64      .00     5.03    30428.
* MODE  32   0   4   3     1467.016       .164    11.99    10.71      .00     5.06    30896.
* MODE  33   0   4   3     1467.362       .162    12.06    10.78      .00     5.09    31347.
* MODE  34   0   4   3     1467.703       .161    12.12    10.85      .00     5.11    31794.
* MODE  35   0   4   3     1468.041       .160    12.18    10.92      .00     5.14    32209.
* MODE  36   0   4   3     1468.379       .164    12.24    10.99      .00     5.16    31494.
* MODE  37   0   4   3     1468.719       .167    12.30    11.06      .00     5.19    31112.
* MODE  38   0   4   3     1469.065       .168    12.36    11.13      .00     5.22    30966.
* MODE  39   0   4   2     1469.416       .170    12.42    11.20      .00     5.24    30918.
* MODE  40   0   4   3     1469.767       .170    12.49    11.27      .00     5.27    30927.
* MODE  41   0   4   3     1470.116       .171    12.55    11.33      .00     5.29    30972.
* MODE  42   0   4   3     1470.464       .171    12.61    11.40      .00     5.32    31042.
* MODE  43   0   4   3     1470.812       .172    12.67    11.47      .00     5.34    31130.
* MODE  44   0   4   3     1471.159       .172    12.73    11.54      .00     5.37    31233.
* MODE  45   0   4   2     1471.505       .172    12.79    11.60      .00     5.40    31346.
* MODE  46   0   4   3     1471.850       .172    12.85    11.67      .00     5.42    31467.
* MODE  47   0   4   3     1472.193       .172    12.91    11.73      .00     5.44    31594.
* MODE  48   0   4   2     1472.535       .172    12.96    11.79      .00     5.47    31726.
* MODE  49   0   4   2     1472.877       .172    13.02    11.86      .00     5.49    31863.
* MODE  50   0   4   2     1473.216       .172    13.08    11.92      .00     5.52    32003.
* MODE  55   0   4   2     1474.895       .172    13.36    12.23      .00     5.63    32727.
```

Figure A-3. (Continued)

* MODE	60	0	4	2	1476.540	.172	13.62	12.52	.00	5.75	33465.
* MODE	65	0	4	2	1478.153	.171	13.88	12.80	.00	5.86	34197.
* MODE	70	0	5	3	1479.735	.171	14.12	13.06	.00	5.96	34911.
* MODE	75	0	5	3	1481.290	.170	14.36	13.32	.00	6.06	35605.
* MODE	80	0	5	2	1482.815	.168	14.59	13.57	.00	6.16	36606.
* MODE	85	0	5	2	1484.285	.164	14.81	13.80	.00	6.25	38130.
* MODE	90	0	5	2	1485.711	.162	15.01	14.02	.00	6.35	39194.
* MODE	95	0	5	2	1487.104	.165	15.21	14.23	.00	6.63	40124.
* MODE	100	0	5	2	1488.468	.168	15.40	14.44	.00	6.90	40973.
* MODE	105	0	5	2	1489.808	.172	15.59	14.64	.00	7.17	41764.
* MODE	110	0	5	2	1491.126	.175	15.77	14.83	.00	7.42	42511.
* MODE	115	0	5	2	1492.424	.178	15.95	15.02	.00	7.67	43219.
* MODE	120	0	5	2	1493.704	.180	16.12	15.20	.00	7.92	43896.
* MODE	125	0	5	2	1494.966	.183	16.28	15.38	.00	8.15	44545.
* MODE	130	0	5	2	1496.213	.186	16.45	15.55	.00	8.38	45169.
* MODE	135	0	5	2	1497.444	.188	16.60	15.72	.00	8.61	45770.
* MODE	140	0	5	2	1498.662	.191	16.76	15.88	.00	8.83	46352.
* MODE	145	0	5	2	1499.867	.193	16.91	16.04	.00	9.05	46914.
* MODE	150	0	5	2	1501.060	.194	17.06	16.20	.00	9.20	47460.
* MODE	155	0	5	2	1502.241	.193	17.21	16.36	.00	9.26	47990.
* MODE	160	0	5	2	1503.412	.192	17.35	16.51	.00	9.32	48505.
* MODE	165	0	6	3	1504.572	.191	17.49	16.66	.00	9.38	49006.
* MODE	170	0	6	3	1505.722	.191	17.63	16.80	.00	9.44	49495.
* MODE	175	0	6	3	1506.889	.190	17.77	16.95	.00	9.50	49982.
* MODE	180	0	6	3	1508.144	.280	17.92	17.10	2.23	12.17	43433.
* MODE	185	0	6	3	1509.498	.312	18.08	17.27	3.30	12.69	40619.

*** SEARCH IS TERMINATED ***   7   186   .1510+04   .1510+04   .1510+04

Figure A-3. (Continued)

SOUND LEVEL. RCV AT	10.0	50.0	200.0	400.0	100.0						
RANGE	SL	SL	SL	SL	SL	SL	SL	SL	SL	SL	SL
RKM 100.000	102.5	103.7	103.7	100.6	103.8						
10 PER-CENT	112.7	114.0	114.0	110.2	114.1						
90 PER-CENT	98.9	100.1	100.2	97.2	100.2						
COHERENT SL	109.1	112.1	115.6	104.6	113.0						
RANDOM 100.000	102.2	103.4	102.8	101.7	102.7						
RKM 100.000	102.5	103.7	103.7	100.6	103.8						
RKM 120.000	107.1	108.4	108.3	105.9	107.6						
10 PER-CENT	117.5	118.8	118.6	115.8	117.7						
90 PER-CENT	103.6	104.9	104.8	102.4	104.1						
COHERENT SL	115.5	124.4	120.8	111.0	113.5						
RKM 140.000	110.9	111.6	110.5	111.5	111.4						
10 PER-CENT	121.1	121.8	119.8	121.8	121.2						
90 PER-CENT	107.4	108.1	107.1	107.9	107.9						
COHERENT SL	117.2	117.6	114.2	124.4	116.0						
RKM 160.000	115.1	116.7	115.8	114.2	115.9						
10 PER-CENT	125.4	127.0	125.9	124.3	126.0						
90 PER-CENT	111.6	113.2	112.3	110.7	112.4						
COHERENT SL	121.5	127.8	121.7	119.8	121.3						
RKM 180.000	117.6	120.6	120.7	117.6	121.3						
10 PER-CENT	126.5	131.0	131.0	127.2	131.6						
90 PER-CENT	114.3	117.1	117.1	114.2	117.7						
COHERENT SL	120.9	130.0	130.4	121.7	134.8						
RKM 200.000	122.7	125.0	125.1	123.6	125.0						
10 PER-CENT	132.6	135.4	135.5	134.0	135.3						
90 PER-CENT	119.2	121.5	121.6	120.0	121.4						
COHERENT SL	127.6	139.1	144.3	138.0	134.6						
RKM 220.000	124.9	128.6	125.8	127.1	126.2						
10 PER-CENT	132.9	138.9	134.0	137.4	134.6						
90 PER-CENT	121.7	125.1	122.6	123.6	123.0						
COHERENT SL	127.5	138.1	128.5	135.9	129.1						

Figure A-3. (Continued)

```
RKM      240.000     130.6     131.6     132.2     131.6     132.3

10 PER-CENT          140.5     141.6     142.5     142.0     142.6
90 PER-CENT          127.1     128.1     128.6     128.0     128.8

 COHERENT 5L         135.8     137.0     139.7     149.3     139.4

RKM      260.000     135.8     136.4     136.1     135.4     136.8

10 PER-CENT          146.1     146.7     146.4     145.8     147.0
90 PER-CENT          132.3     132.9     132.5     131.8     133.3

 COHERENT 5L         148.3     146.2     143.7     151.3     148.3

RKM      280.000     138.0     139.7     140.1     138.9     140.0

10 PER-CENT          147.7     150.0     150.5     149.2     150.4
90 PER-CENT          134.5     136.2     136.6     135.4     136.5

 COHERENT SL         142.4     146.6     149.0     149.4     147.2

RKM      300.000     142.2     143.3     143.7     141.3     144.5

10 PER-CENT          152.2     153.5     154.1     151.1     154.7
90 PER-CENT          138.7     139.8     140.2     137.8     140.9

 COHERENT SL         147.4     149.5     151.6     145.9     156.3


RANDOM   300.000     142.3     143.5     143.1     141.9     142.9

 RKM     300.000     142.2     143.3     143.7     141.3     144.5
DATA IGNORED - IN CONTROL MODE


@FIN
```

Figure A-3. (Continued)